Coastal-Urban Boundary layer characteristics

P. Ramamurthy, J. Gonzalez, K. Rahman, H. Gamarro, G. Rios & O. Addasi | CUNY City College | Dep. Mech. Eng.

The City College of New York

CUBE

Convective-cloud Urban Boundary-layer Experiment

(Jointly conducted during TRACER)

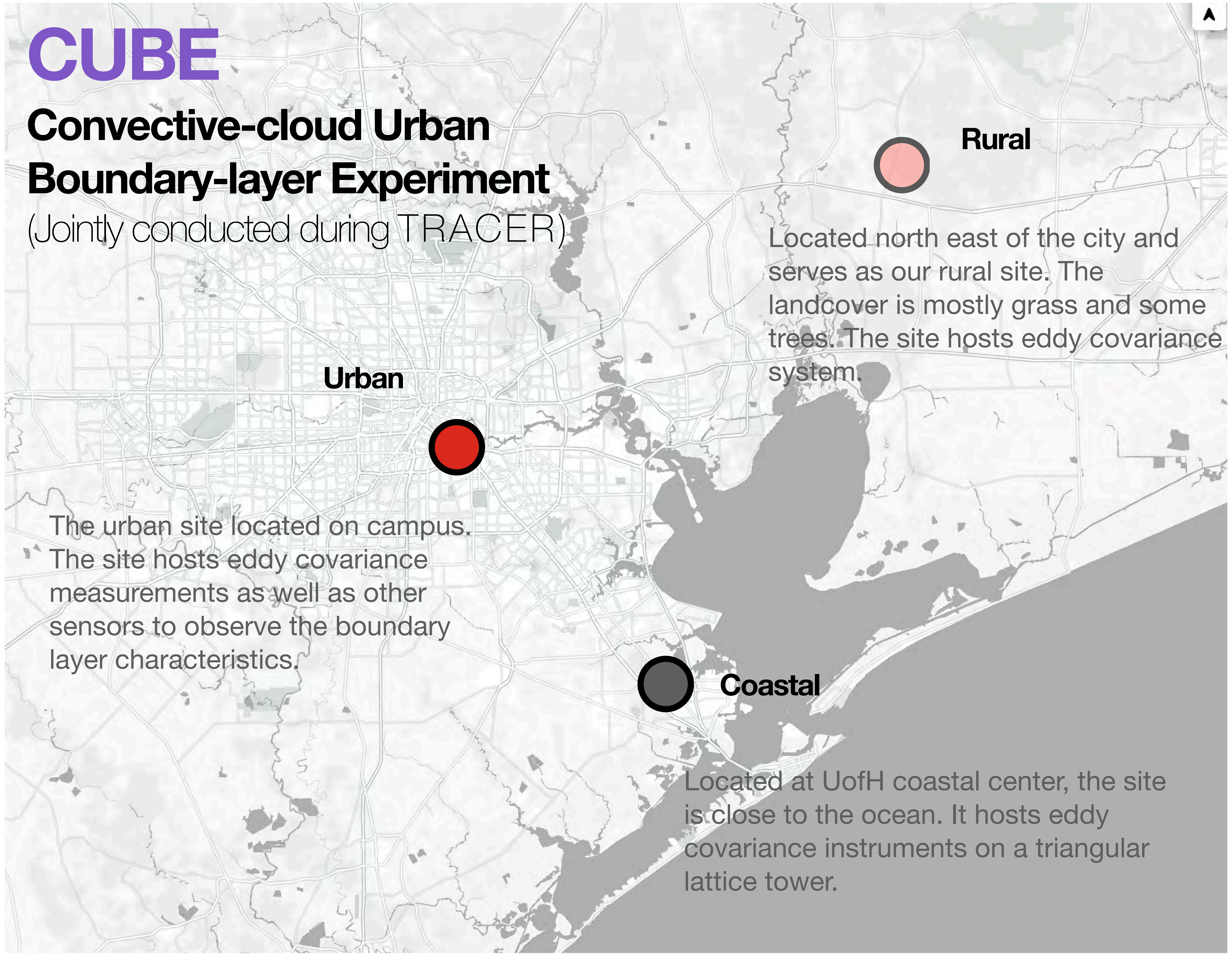

Located north east of the city and serves as our rural site. The landcover is mostly grass and some trees. The site hosts eddy covariance system.

The urban site located on campus. The site hosts eddy covariance measurements as well as other sensors to observe the boundary layer characteristics.

Located at UofH coastal center, the site is close to the ocean. It hosts eddy covariance instruments on a triangular lattice tower.

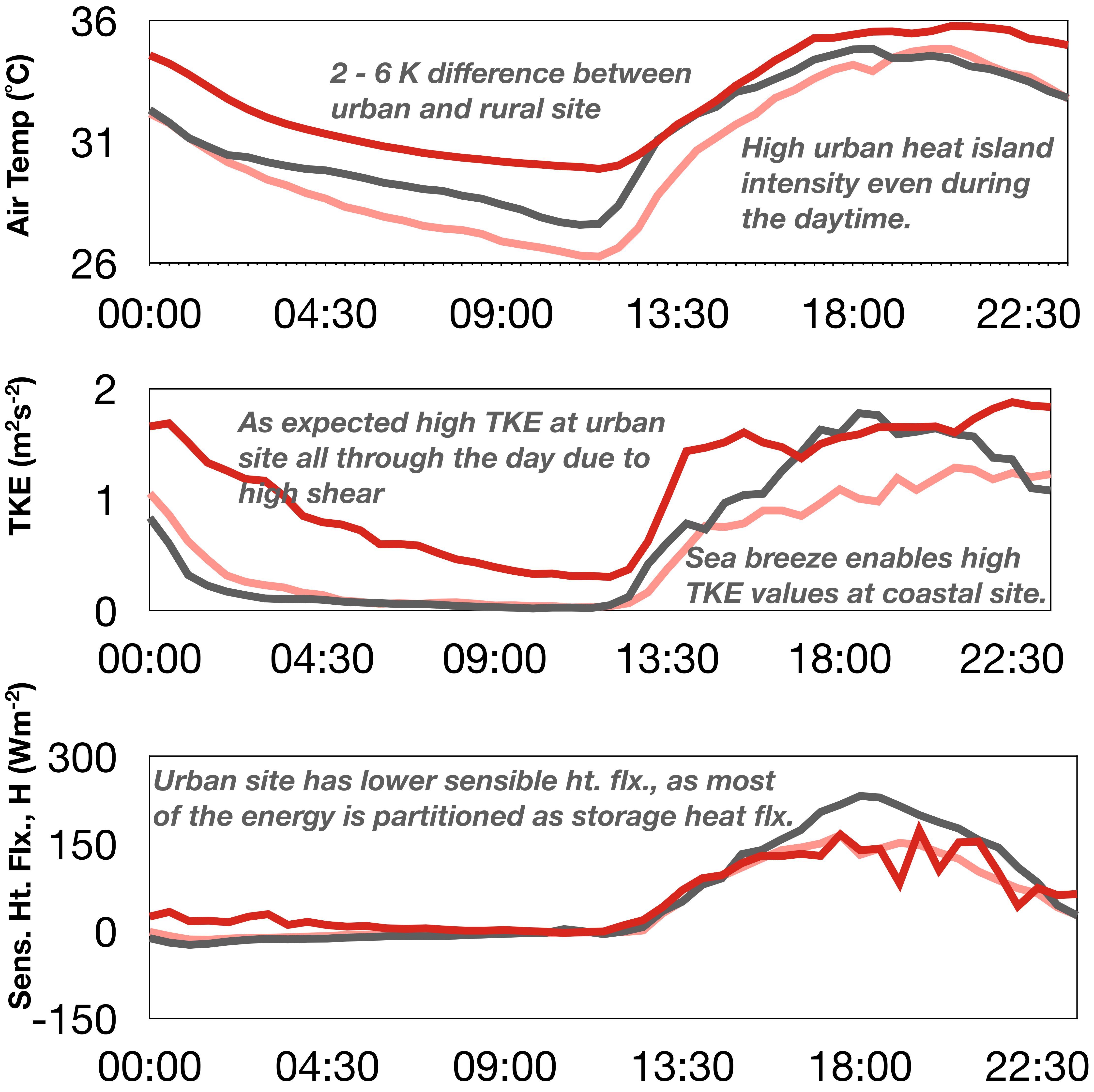

Half-hour averaged daily variability for July 2022. Time in UTC

NSF Funded, AGS 2114198

Boundary layer characteristics

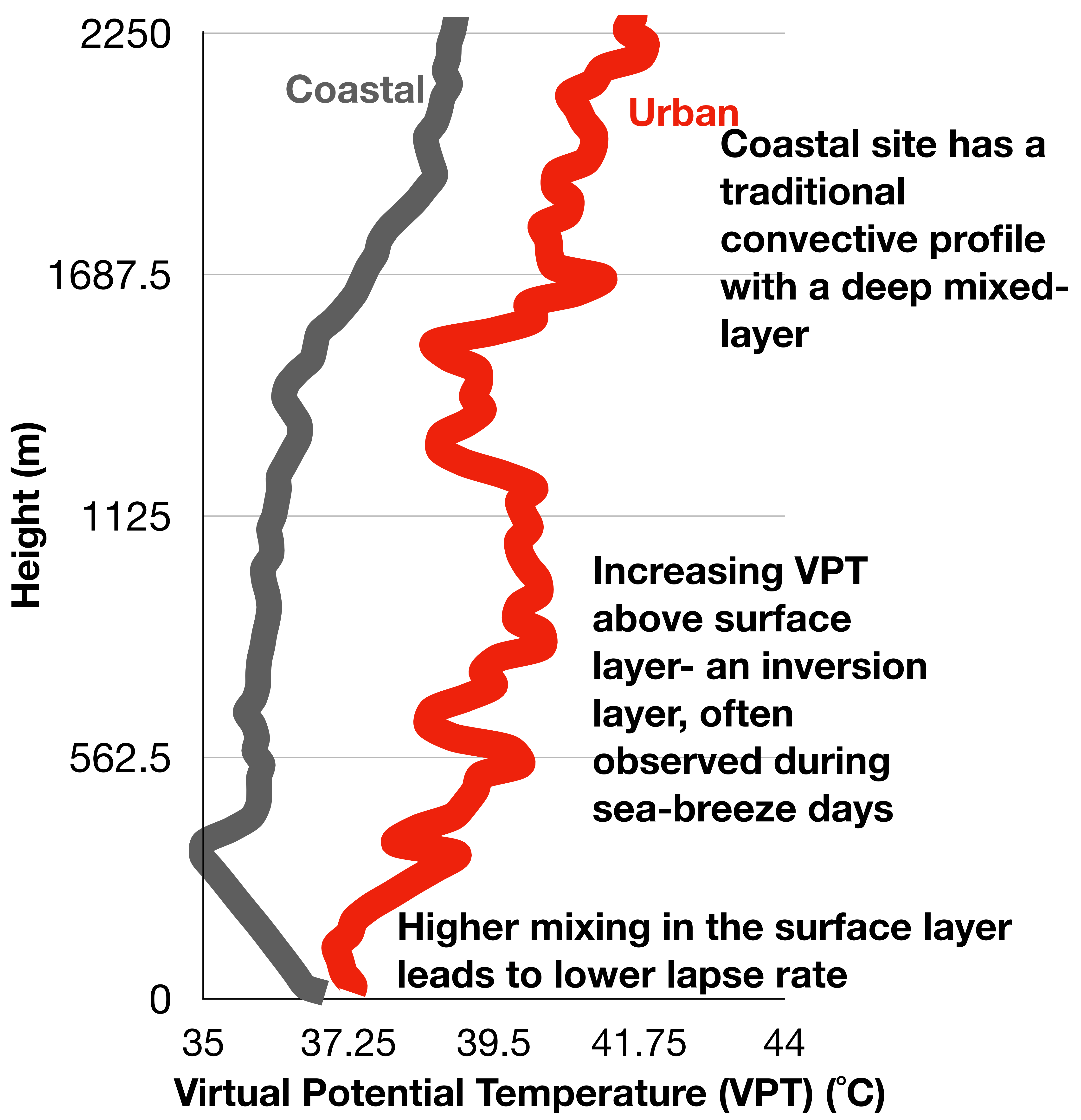

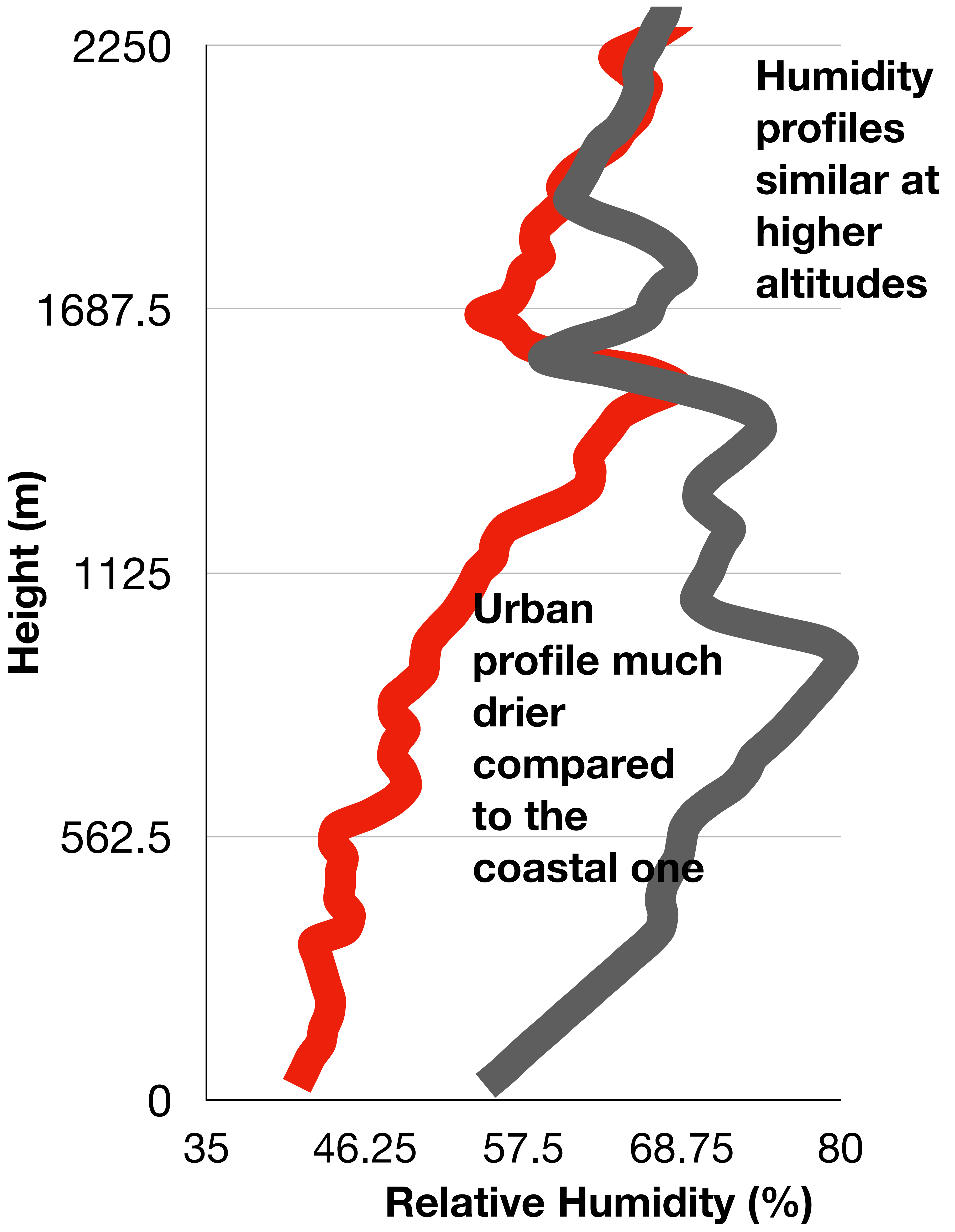

Coastal-Urban Transect

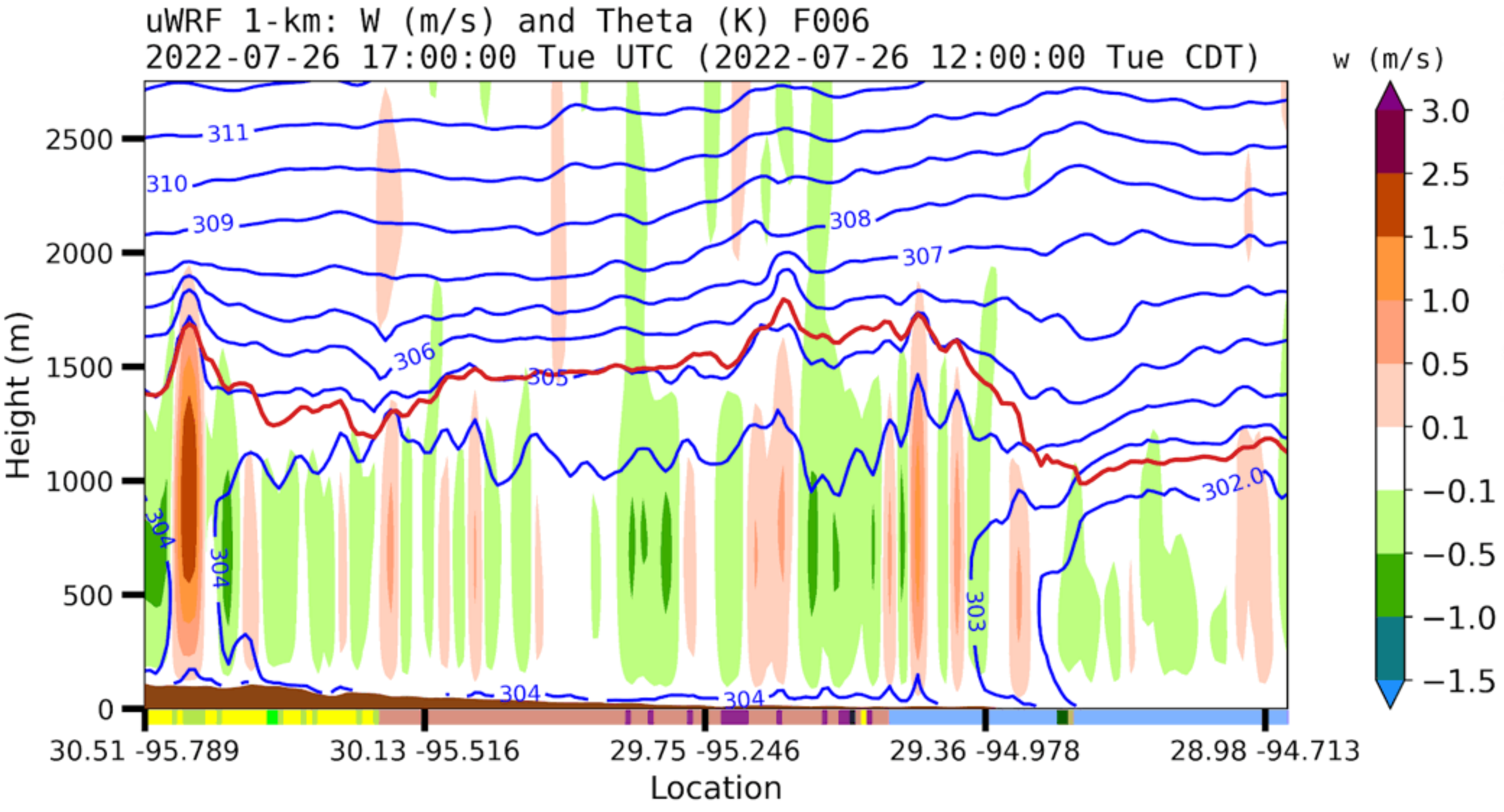

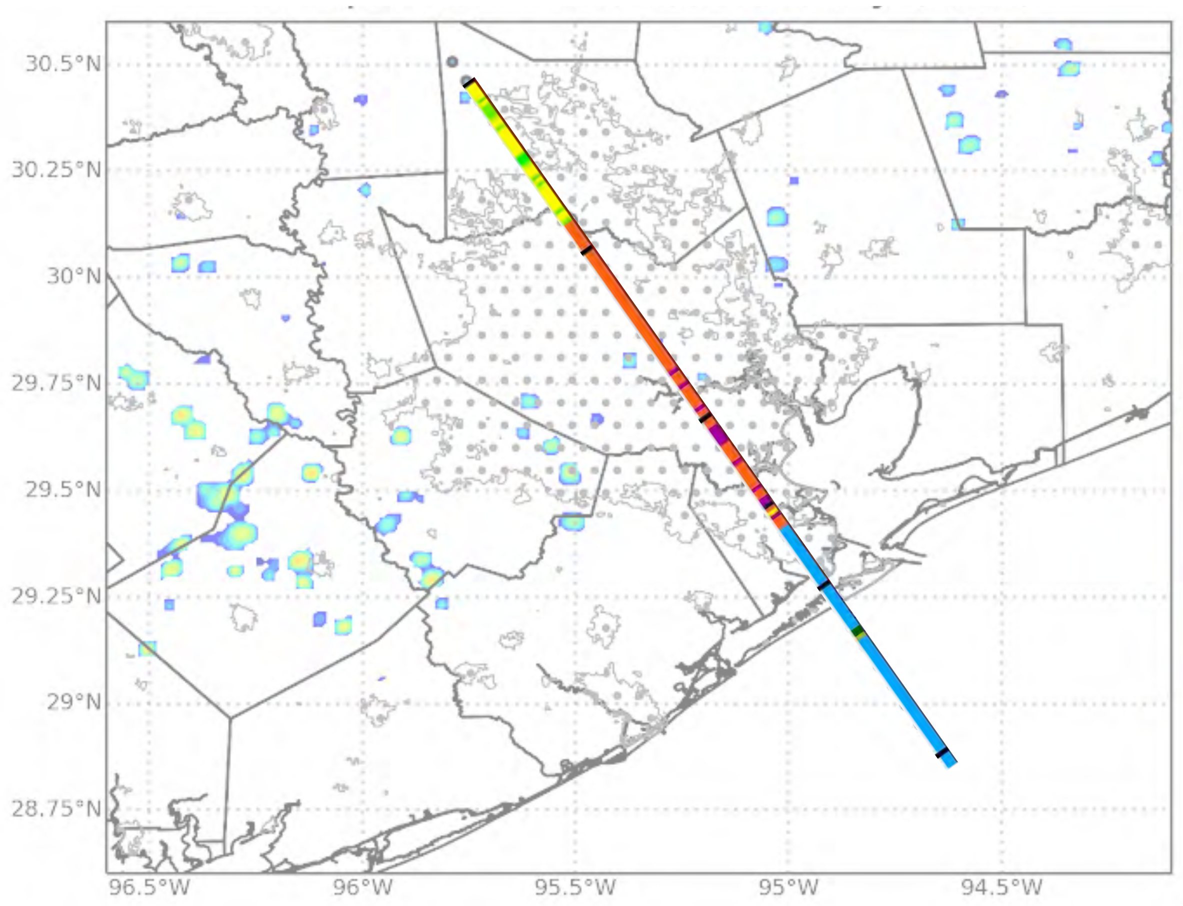

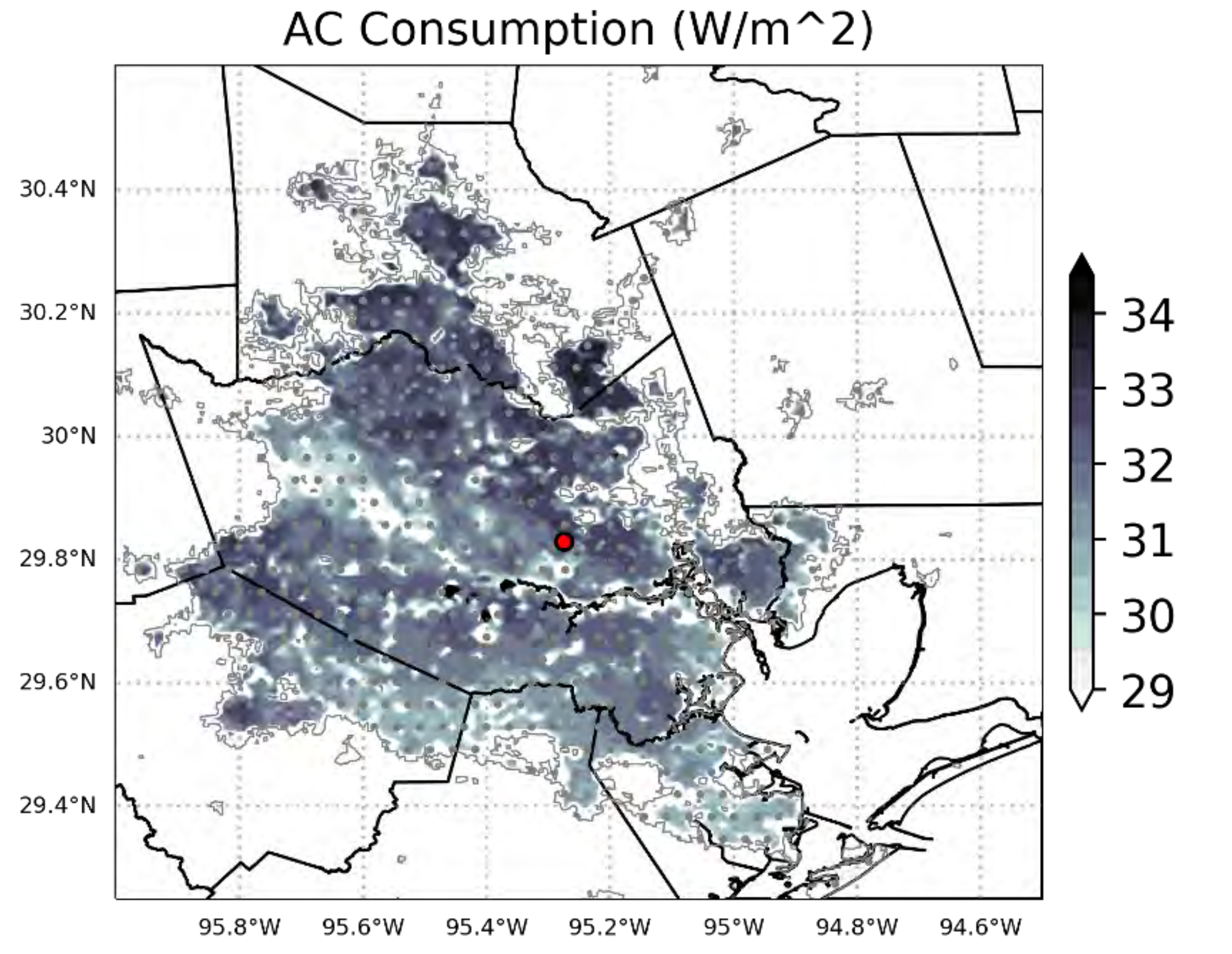

High updrafts observed during the convective period in the urban core. The nocturnal boundary layer over land falls to less than 400 m while during the daytime reaches a peak of around 2500 m. High anthropogenic heat contribution through A/C use.

Stochastic generation of heterogeneous patterns representing natural landscapes

Zun Yin
Program in Atmospheric and Oceanic Sciences, Princeton University

WBLP WG Oct-27-2022

Surface heterogeneity in land-atmosphere interactions

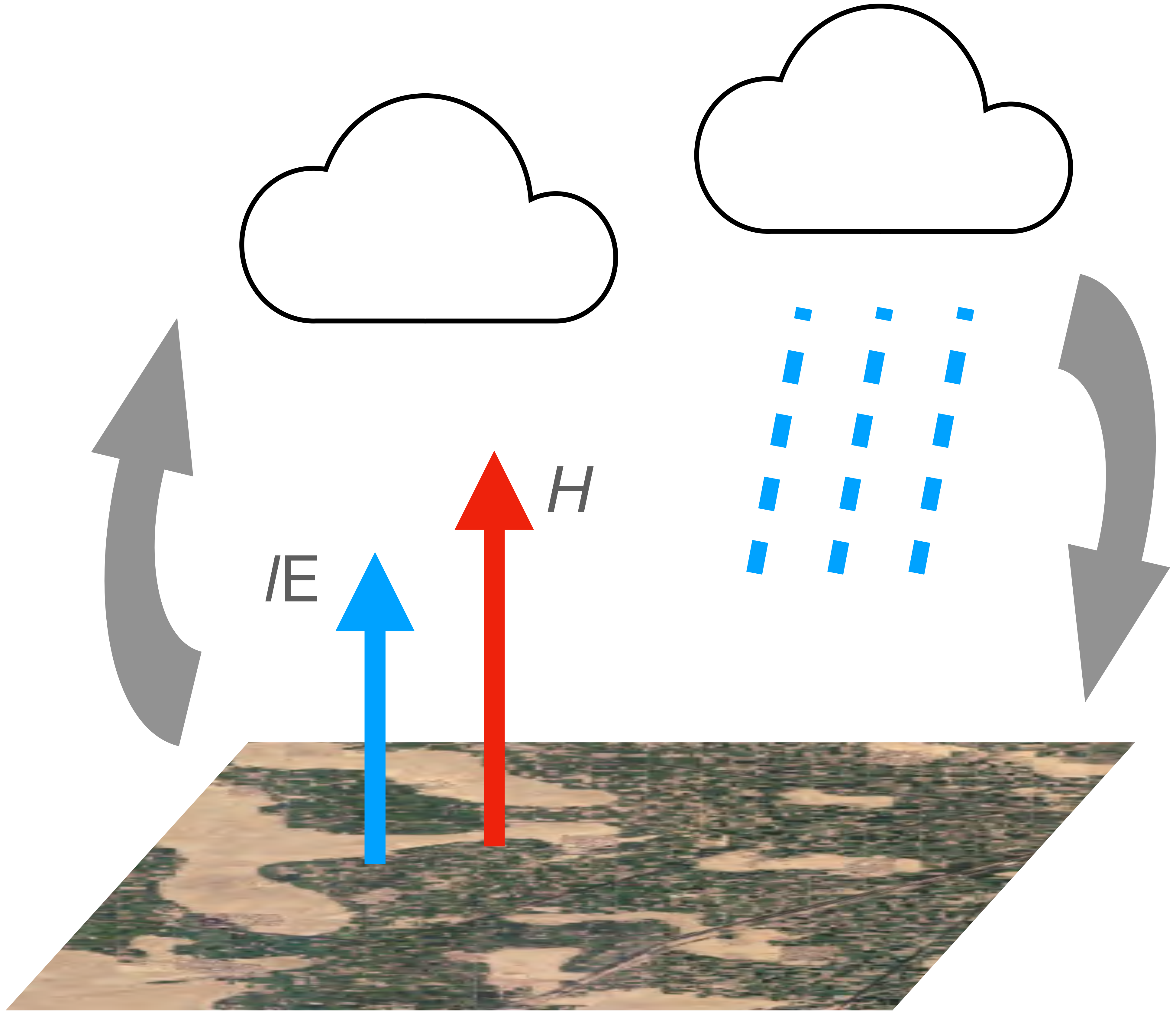

L-A Interactions over heterogeneous surface

Surface heterogeneity in land-atmosphere interactions

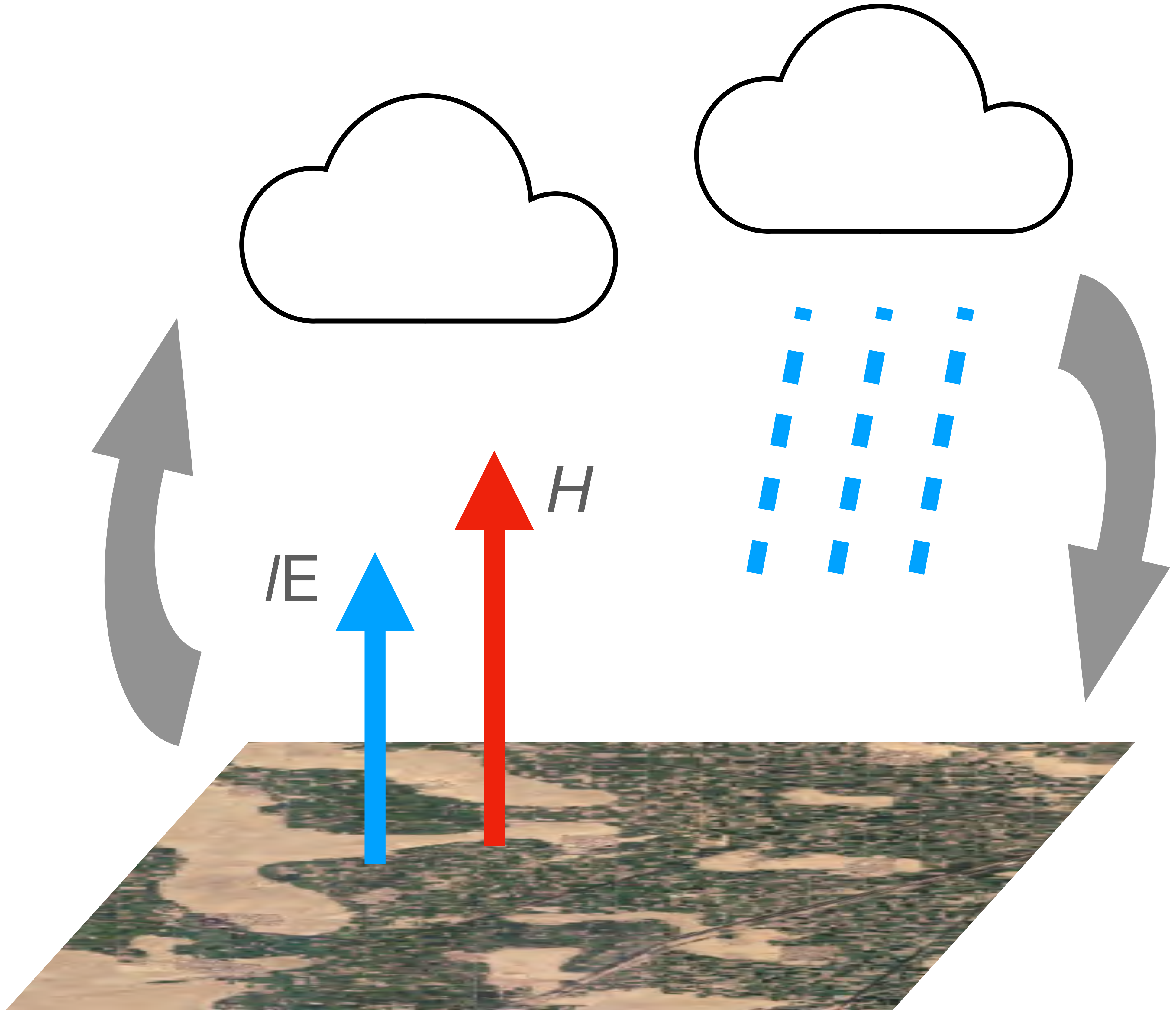

L-A Interactions over heterogeneous surface

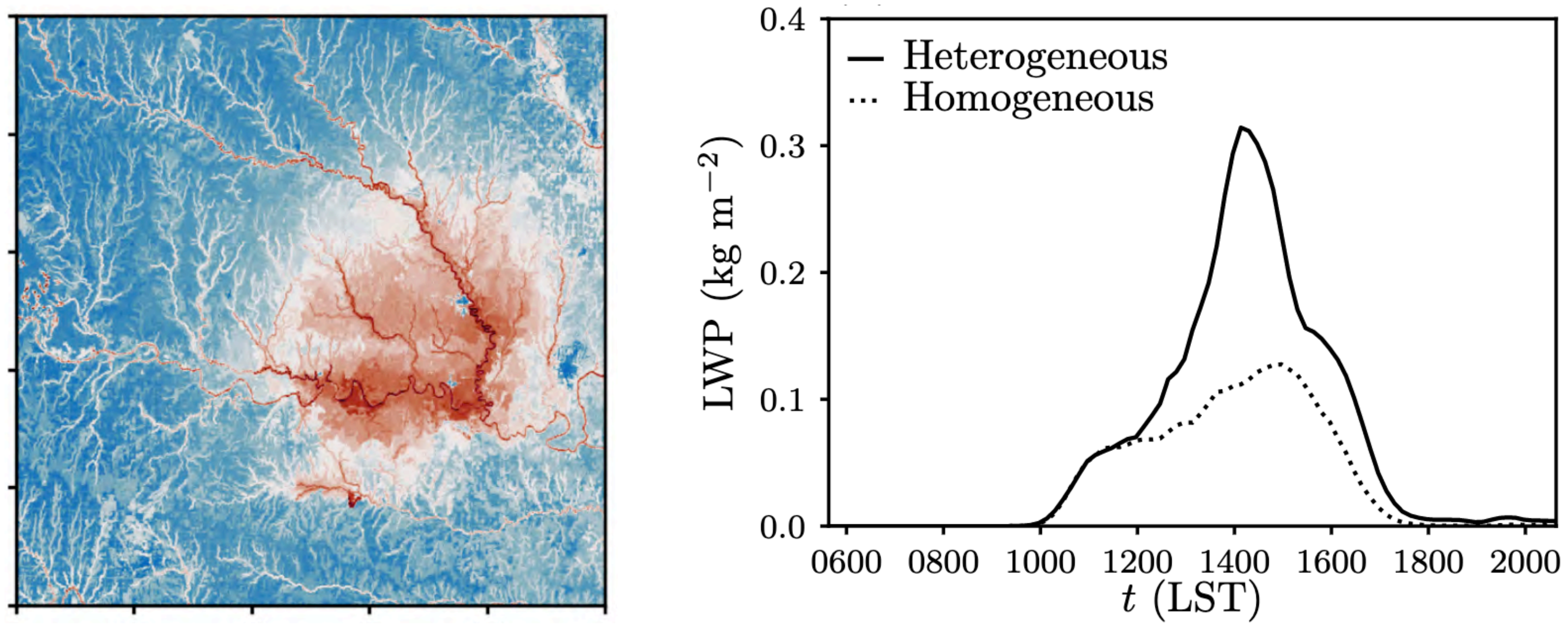

A case study over the Great South Plain
by LES simulations (Simon et al., 2021 JAMES)

Surface heterogeneity in land-atmosphere interactions

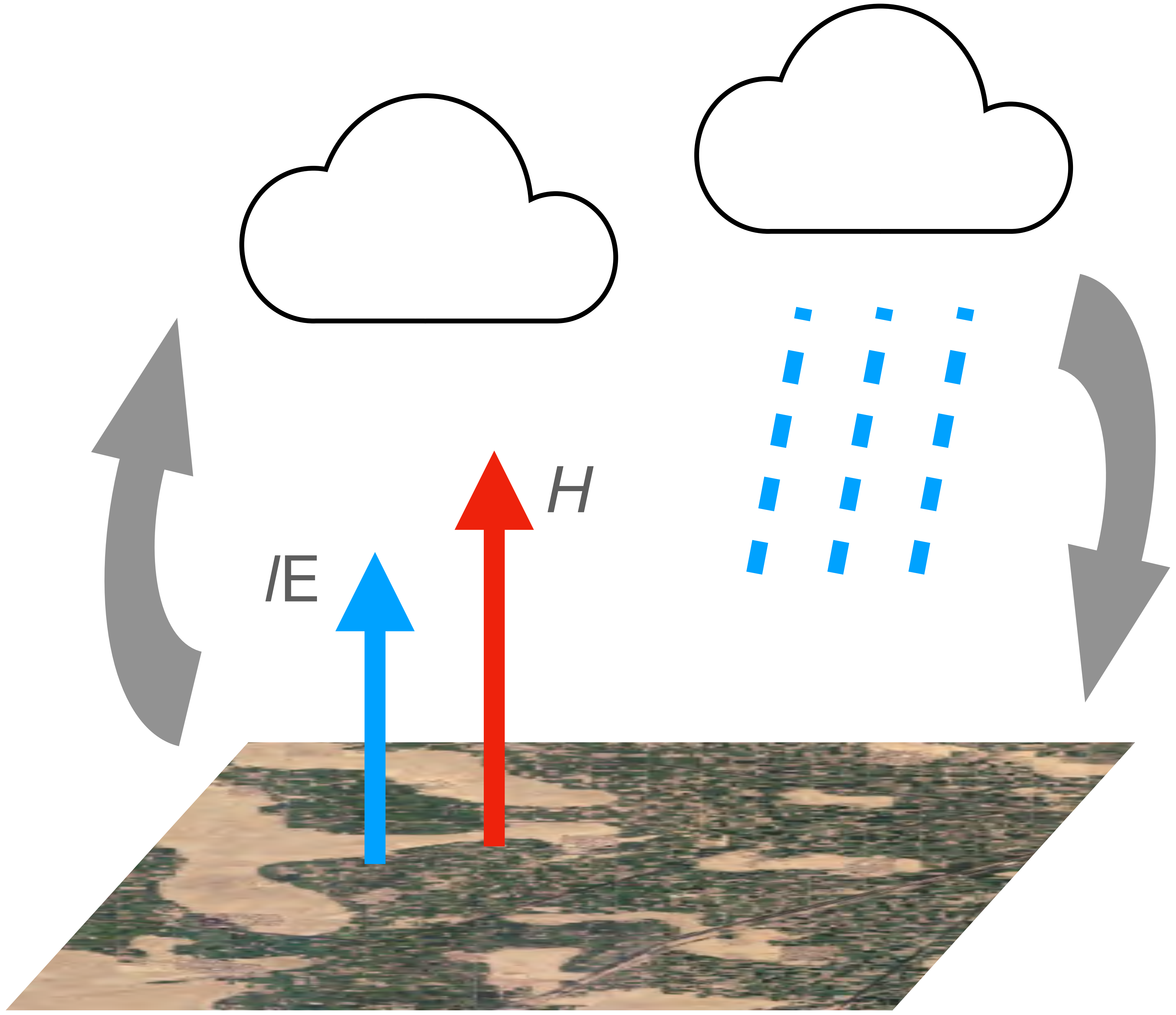

L-A Interactions over heterogeneous surface

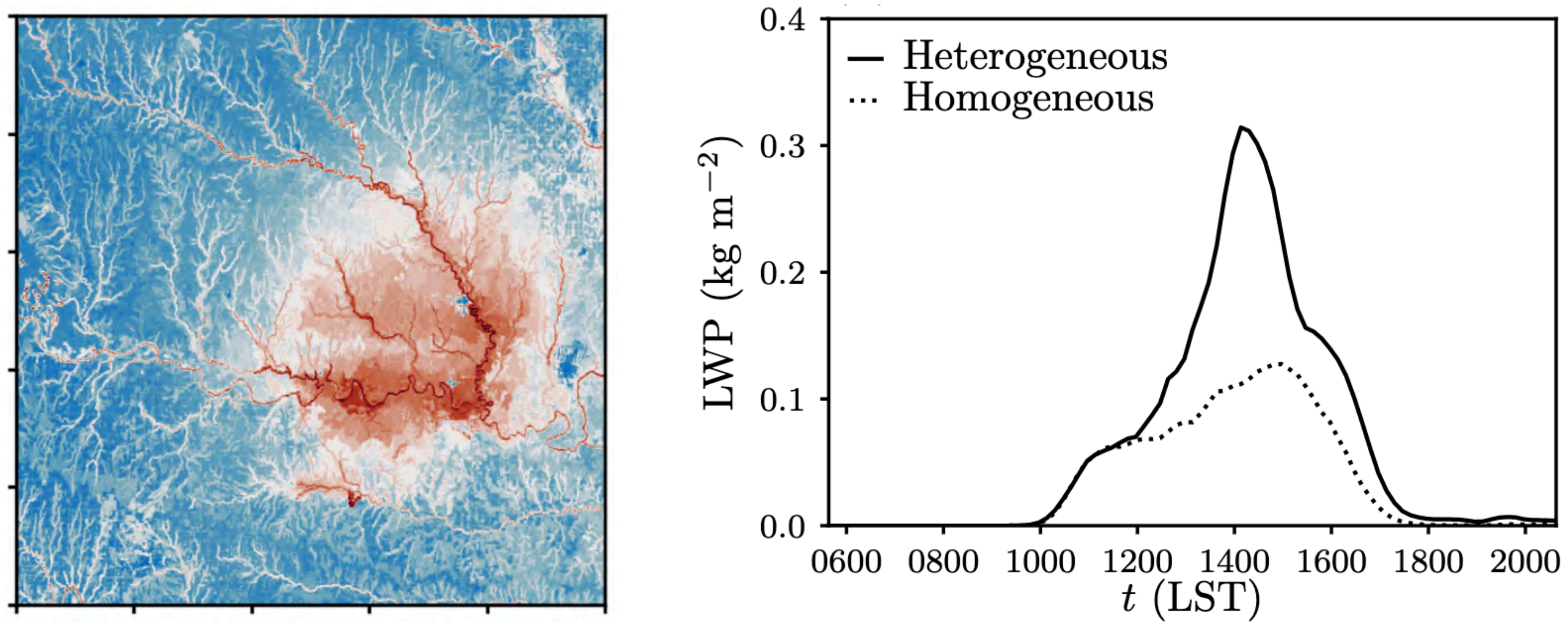

A case study over the Great South Plain
by LES simulations (Simon et al., 2021 JAMES)

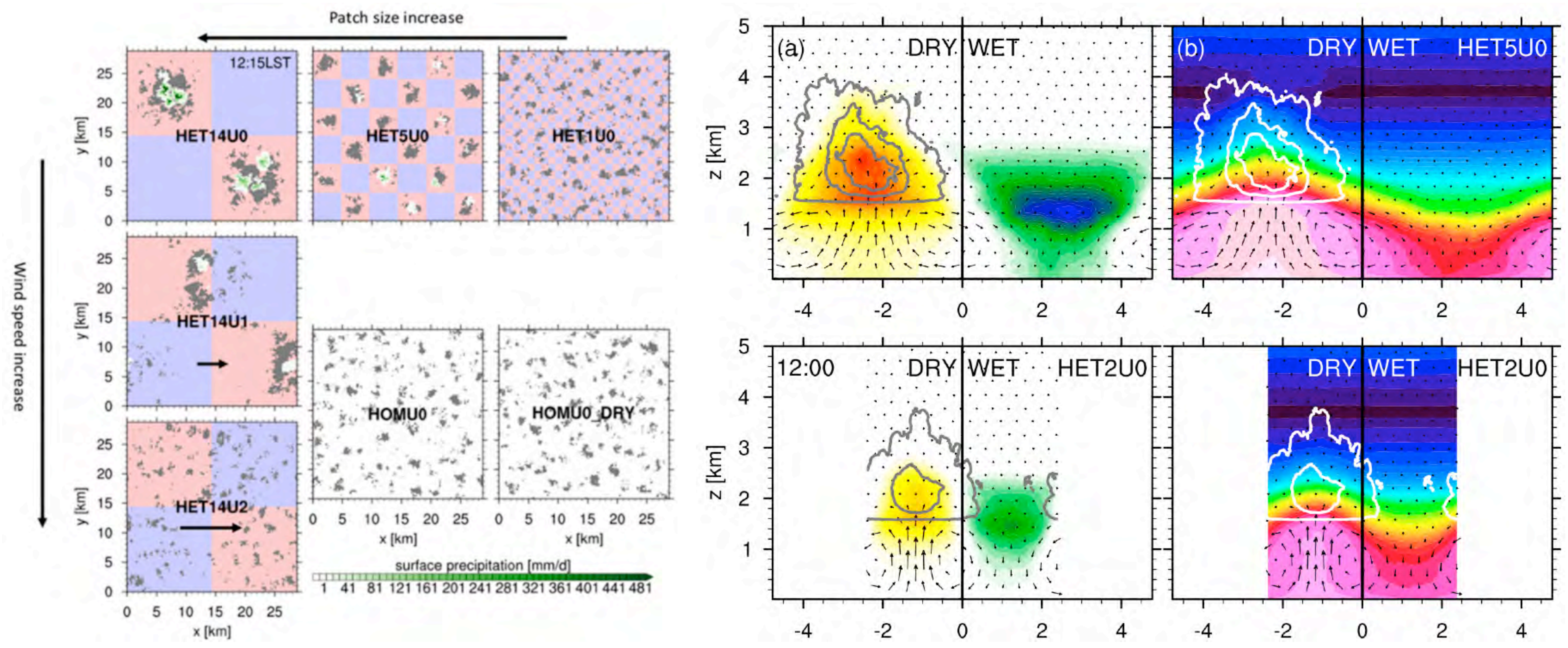

A conceptual study based on LES
simulations (Lee et al., 2019 JAS)

Attribution of heterogeneity impacts to different features

Case studies

- Fixed surface
- Highly coupled features

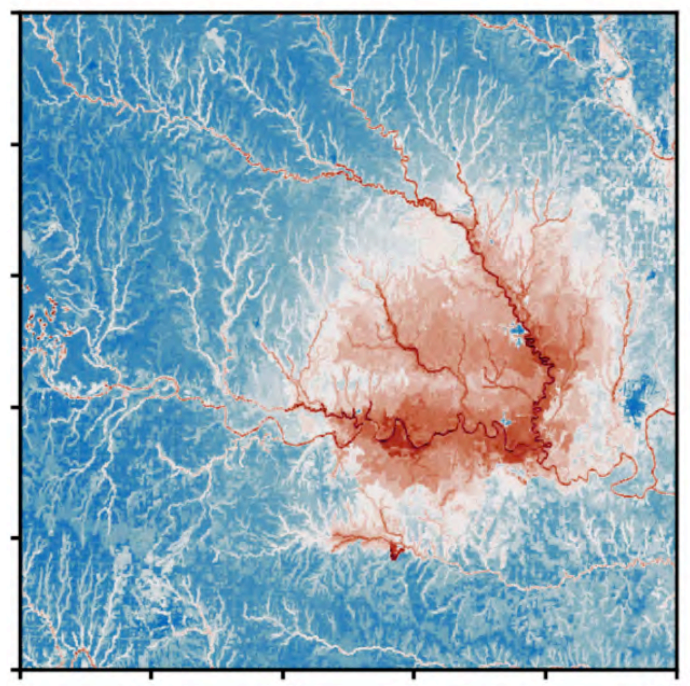

Attribution of heterogeneity impacts to different features

Case studies

- Fixed surface
- Highly coupled features

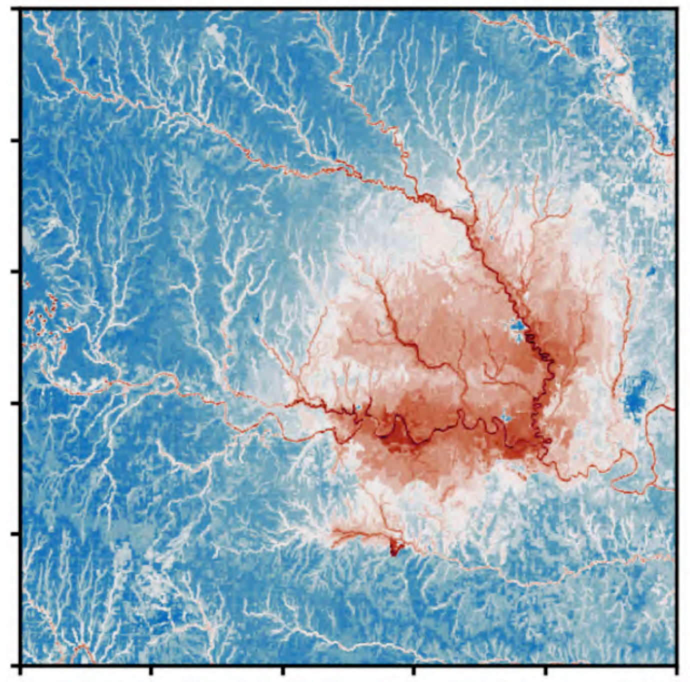

Conceptual studies

- Idealized patterns
- Missing features

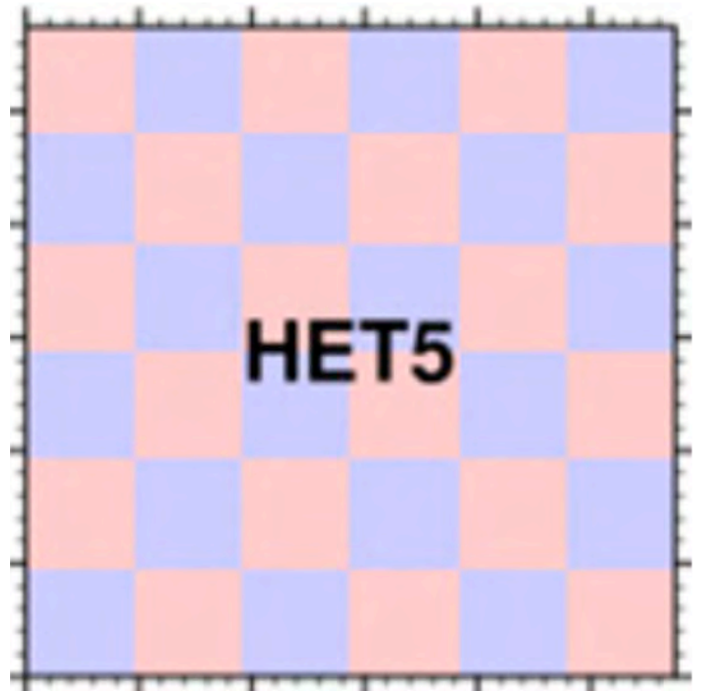

Attribution of heterogeneity impacts to different features

Case studies

- Fixed surface
- Highly coupled features

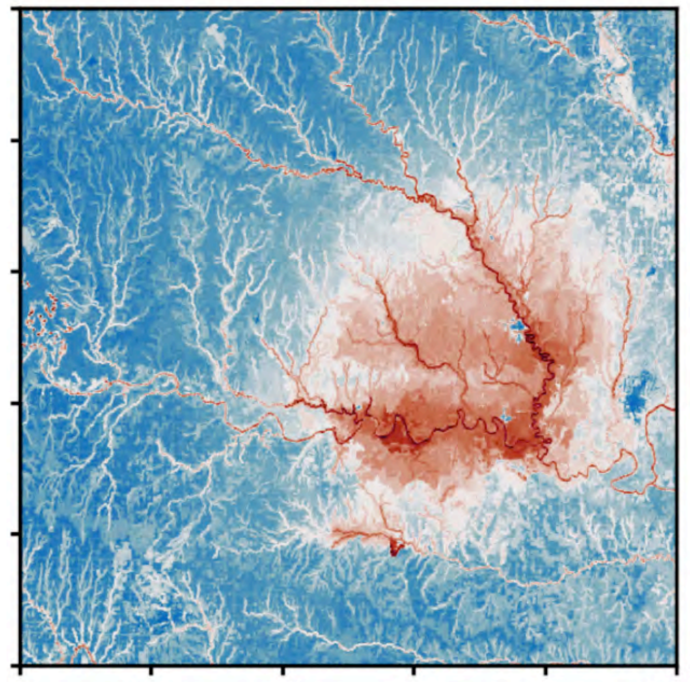

Conceptual studies

- Idealized patterns
- Missing features

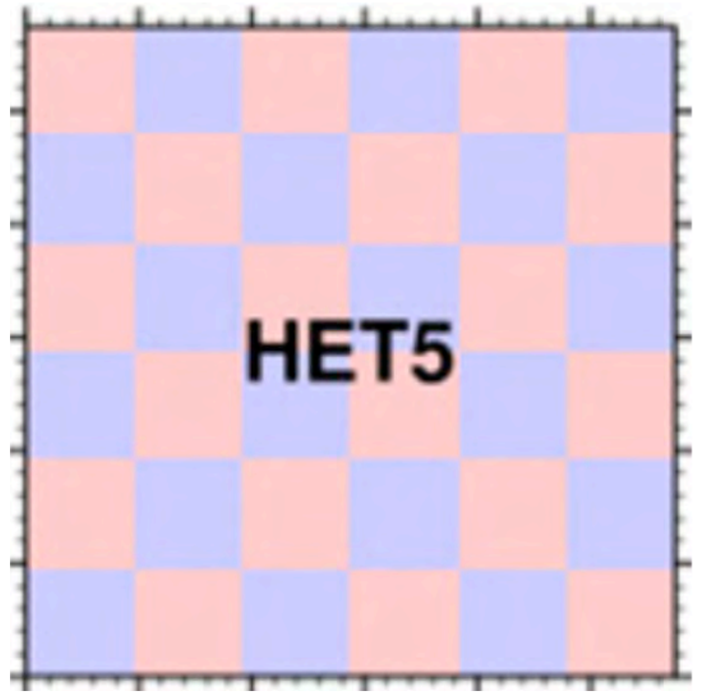

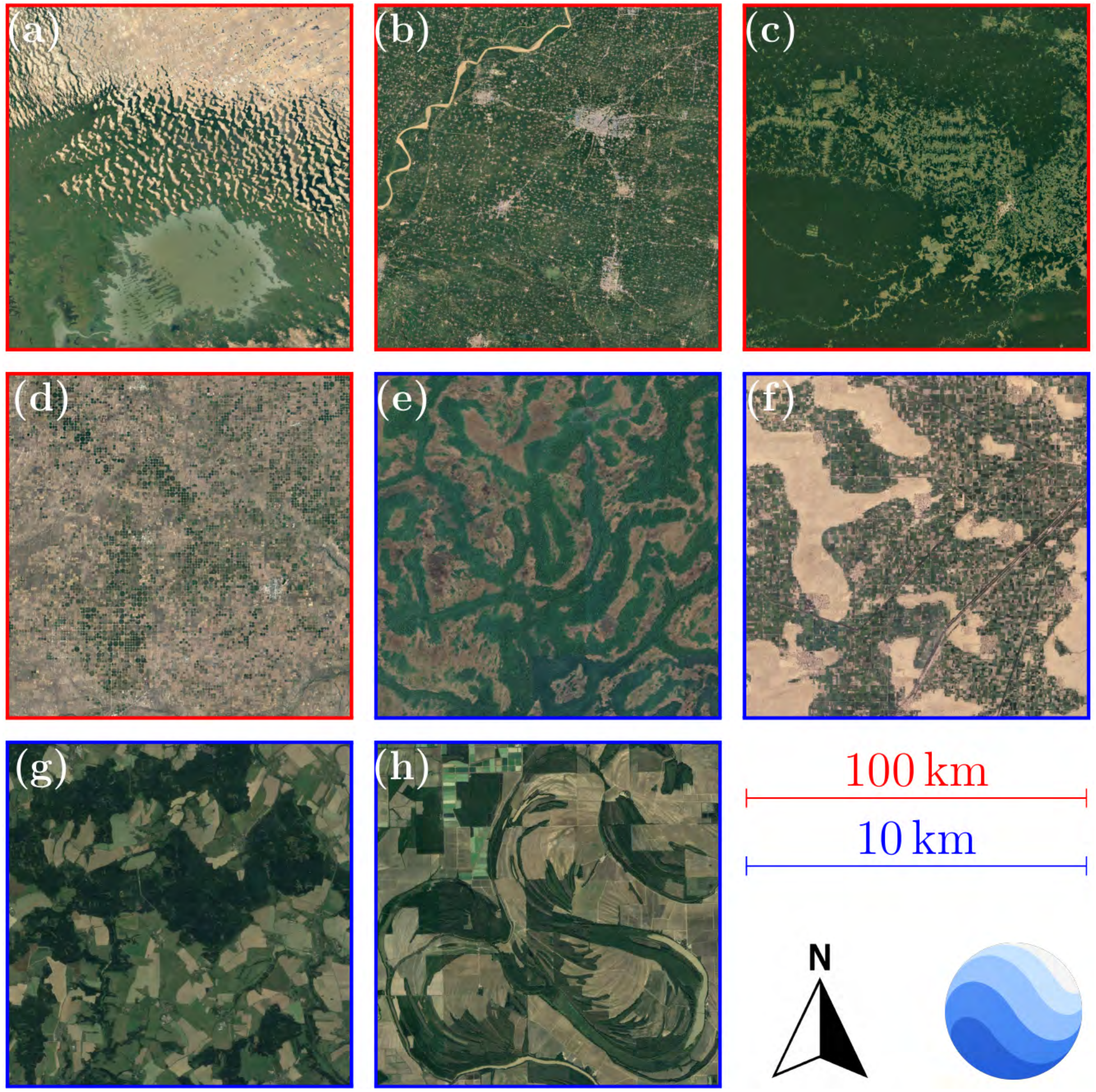

Heterogeneous patterns derived from the Google Earth

Attribution of heterogeneity impacts to different features

A simple approach (e.g., quantifying feature *a*)

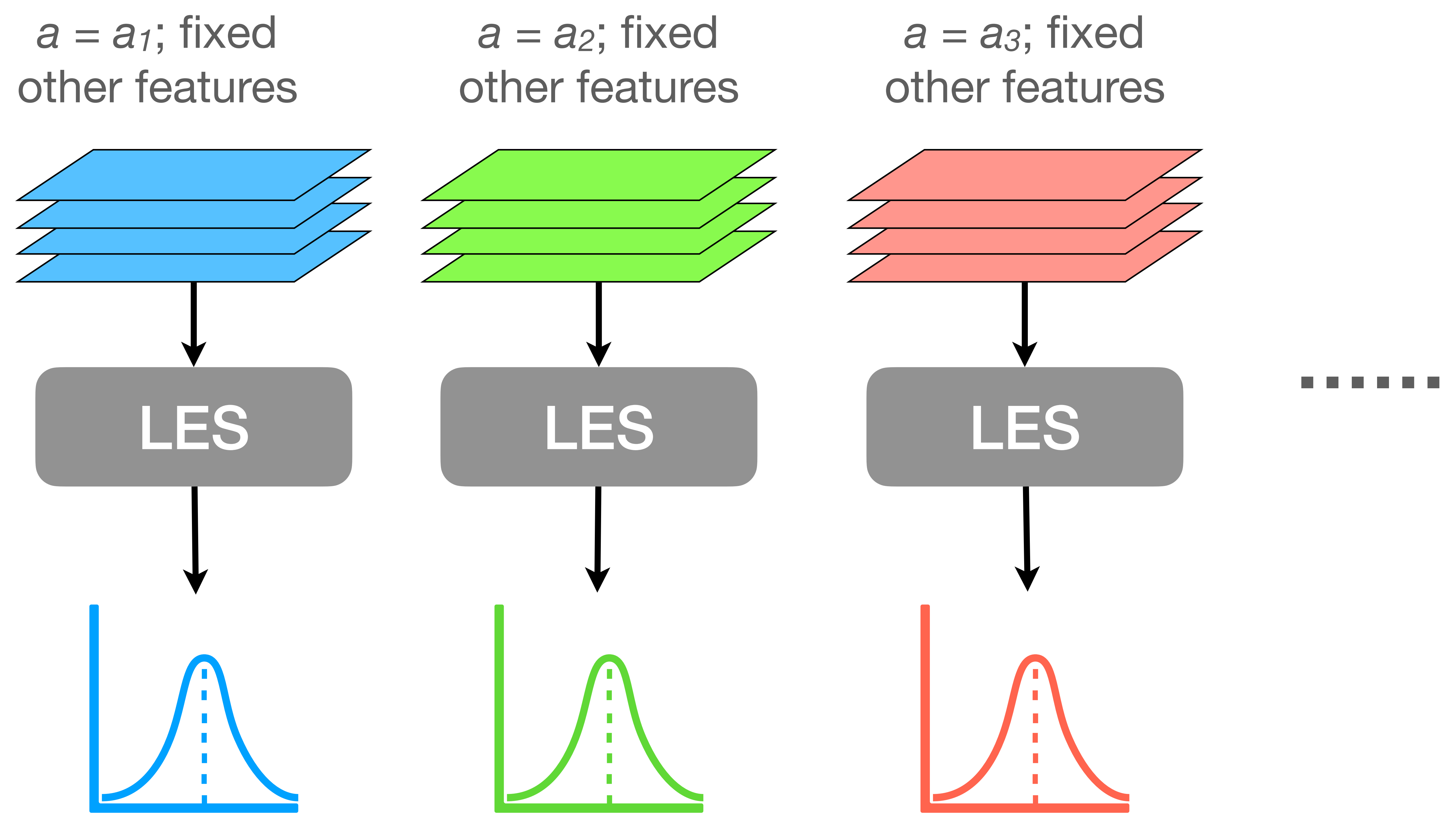

Attribution of heterogeneity impacts to different features

A simple approach (e.g., quantifying feature *a*)

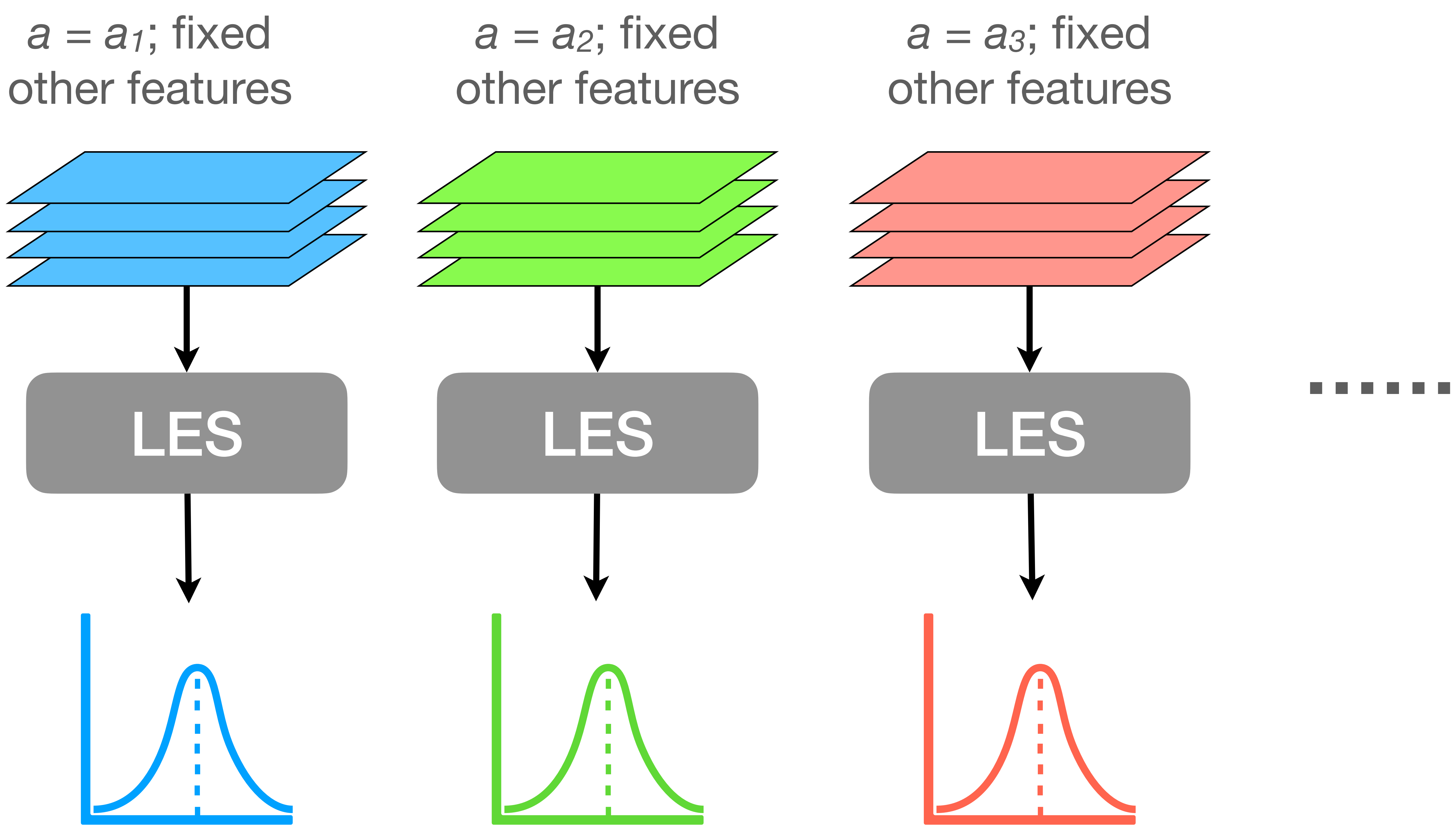

Prerequisites

1. Understanding key heterogeneity features
2. Getting patterns with specific features
3. Spatial independence of patterns within a cluster

Heterogeneity features & Modified Conway's Game of Life (MCGL)

Three key features

- Spatial mean (*M*)
- Standard deviation (*S*)
- **Clustering**
  - Moran's *I* (*I*)

$$I = \frac{K}{\sum_{i,j} g_{i,j}} \cdot \frac{\sum_{i,j} g_{i,j} \left(x_i - \bar{x}\right) \left(x_j - \bar{x}\right)}{\sum_{i} \left(x_i - \bar{x}\right)^2} .$$

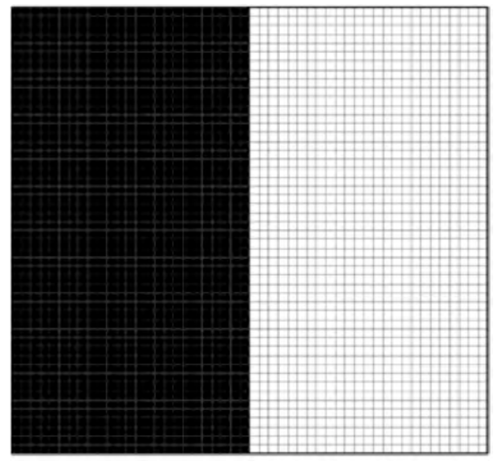

I = -1

I = 0

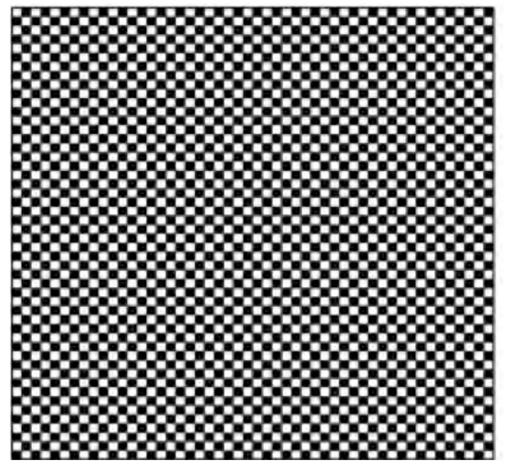

I = 1

Heterogeneity features & Modified Conway's Game of Life (MCGL)

Three key features

- Spatial mean (*M*)
- Standard deviation (*S*)
- **Clustering**
  - Moran's *I* (*I*)

$$I = \frac{K}{\sum_{i,j} g_{i,j}} \cdot \frac{\sum_{i,j} g_{i,j}\left(x_i - \bar{x}\right)\left(x_j - \bar{x}\right)}{\sum_i \left(x_i - \bar{x}\right)^2}.$$

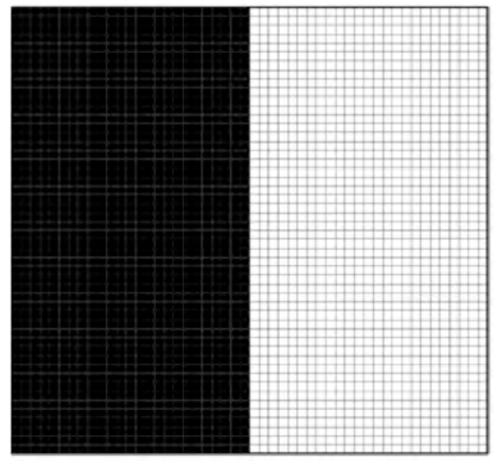

I = -1

I = 0

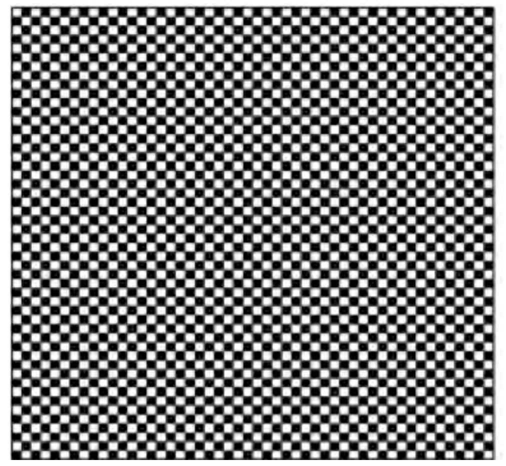

I = 1

MCGL

This model is established by employing the reaction-diffusion system discovered by Alan Turing to Conway's Game of Life.

John Conway

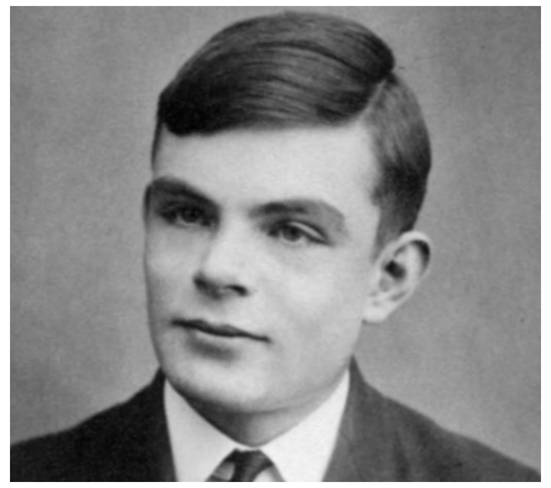

Alan Turing

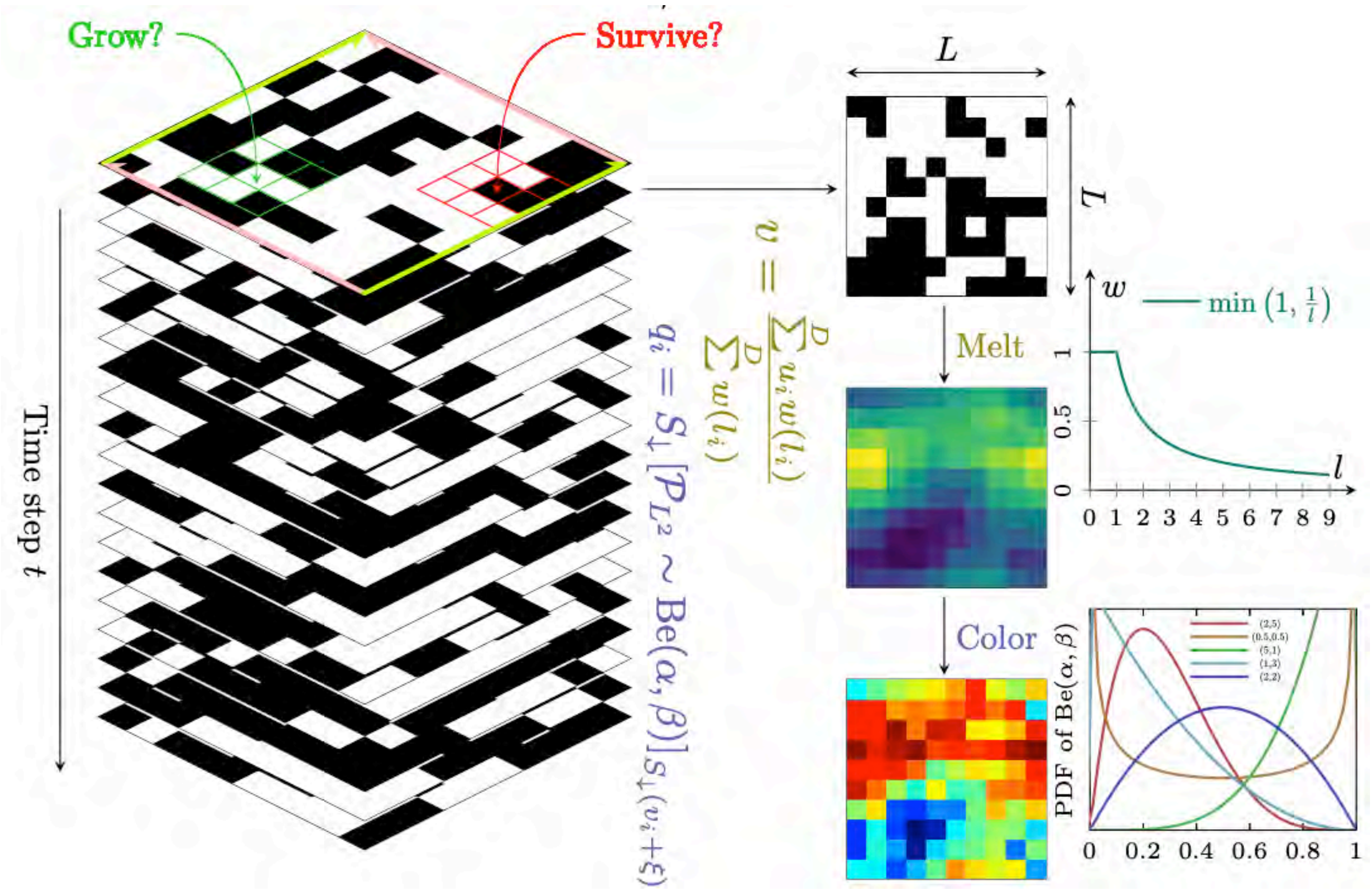

Advantages of MCGL

- **Stability:** One simulation generates numerous patterns with the same features

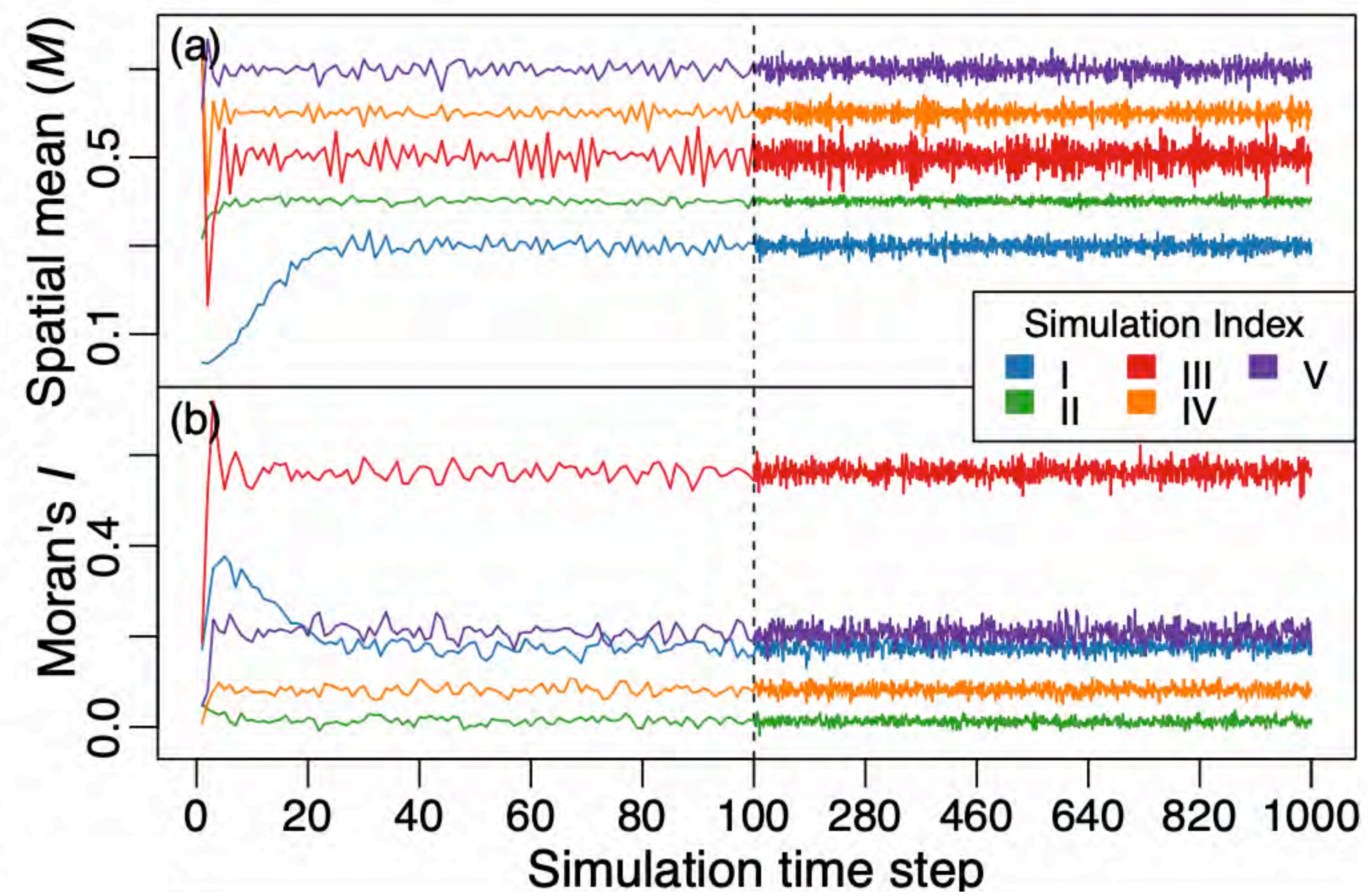

Advantages of MCGL

- **Stability:** One simulation generates numerous patterns with the same features

- **Independence:** Patterns from the same simulation have low spatial correlations.

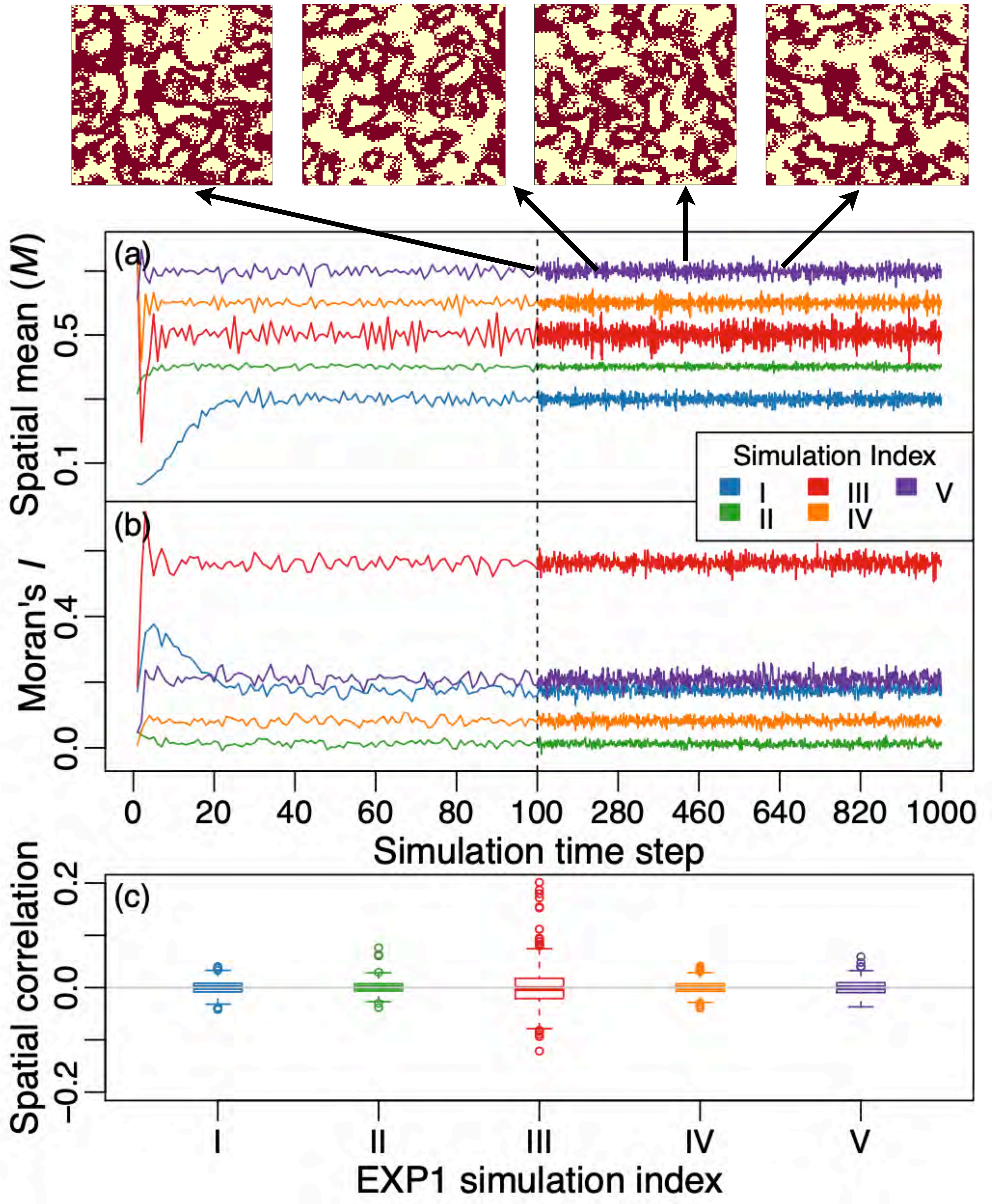

Advantages of MCGL

- **Stability:** One simulation generates numerous patterns with the same features
- **Independence:** Patterns from the same simulation have low spatial correlations.
- **Broad coverage:** MCGL can generate patterns with $0.28 \le M \le 0.7$ and $0 \le I \le 0.71$.

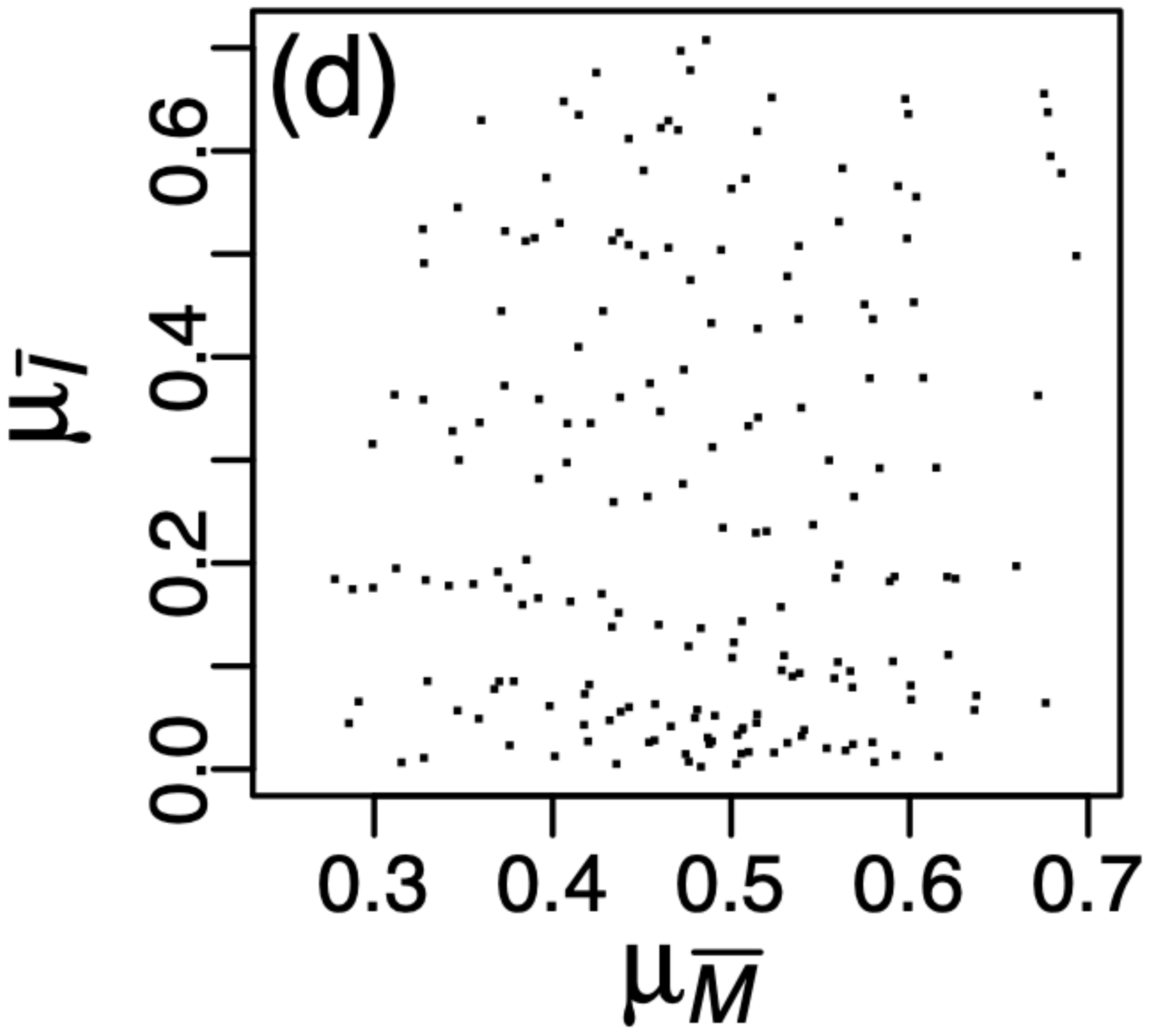

Advantages of MCGL

- **Stability:** One simulation generates numerous patterns with the same features
- **Independence:** Patterns from the same simulation have low spatial correlations.
- **Broad coverage:** MCGL can generate patterns with $0.28 \leq M \leq 0.7$ and $0 \leq I \leq 0.71$.
- **Reproducibility:** Pattern features are determined by parameters, not by the initial states.

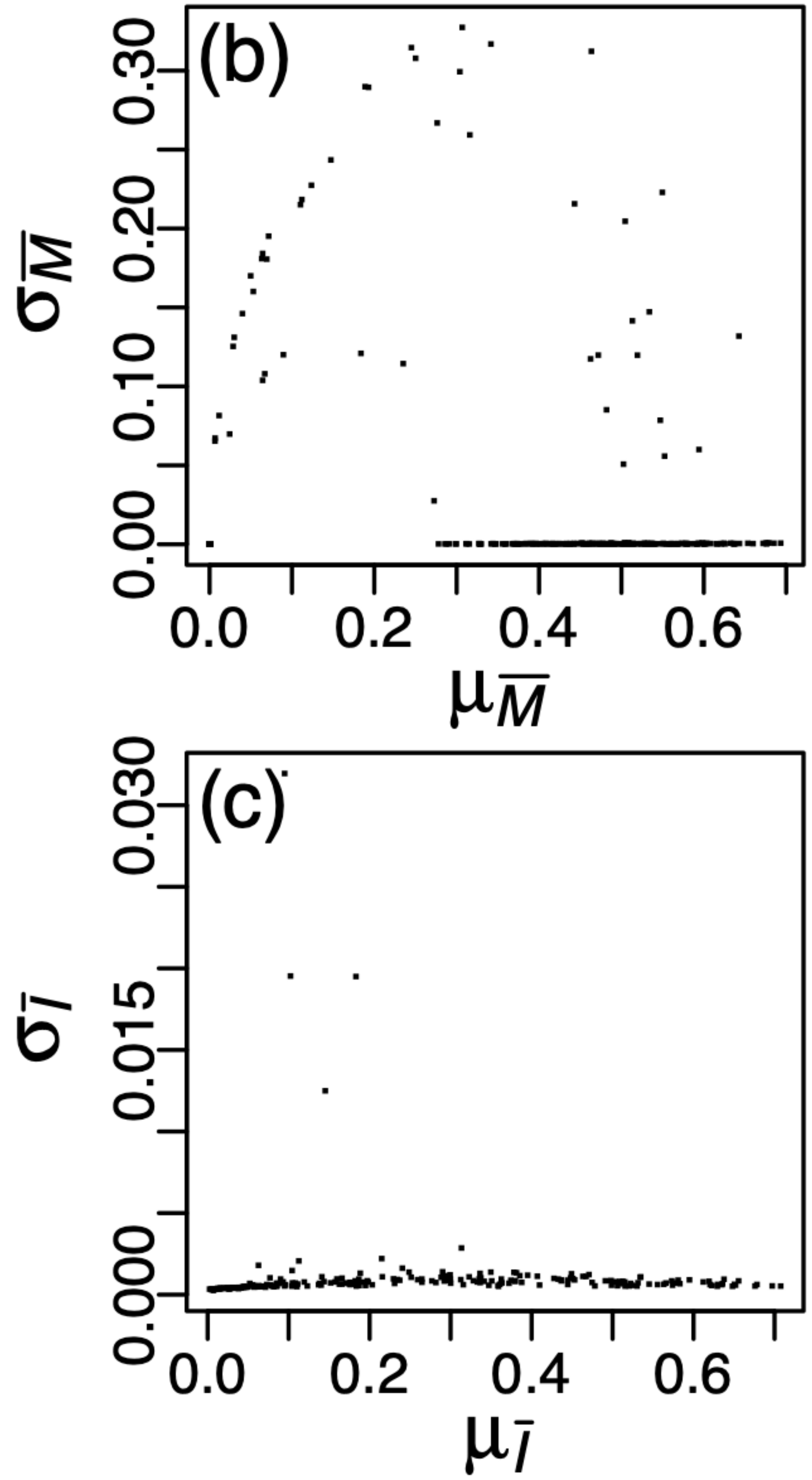

Spatial Variability of Convective Mixing Layer at the SGP Supersite

Z. Wang[1](Zhien.wang@Colorado.edu), L. Xue[2], Y. Chu[1], H. H. Shin[2], and W. Li[2], 1- CU-Boulder, 2- NCAR

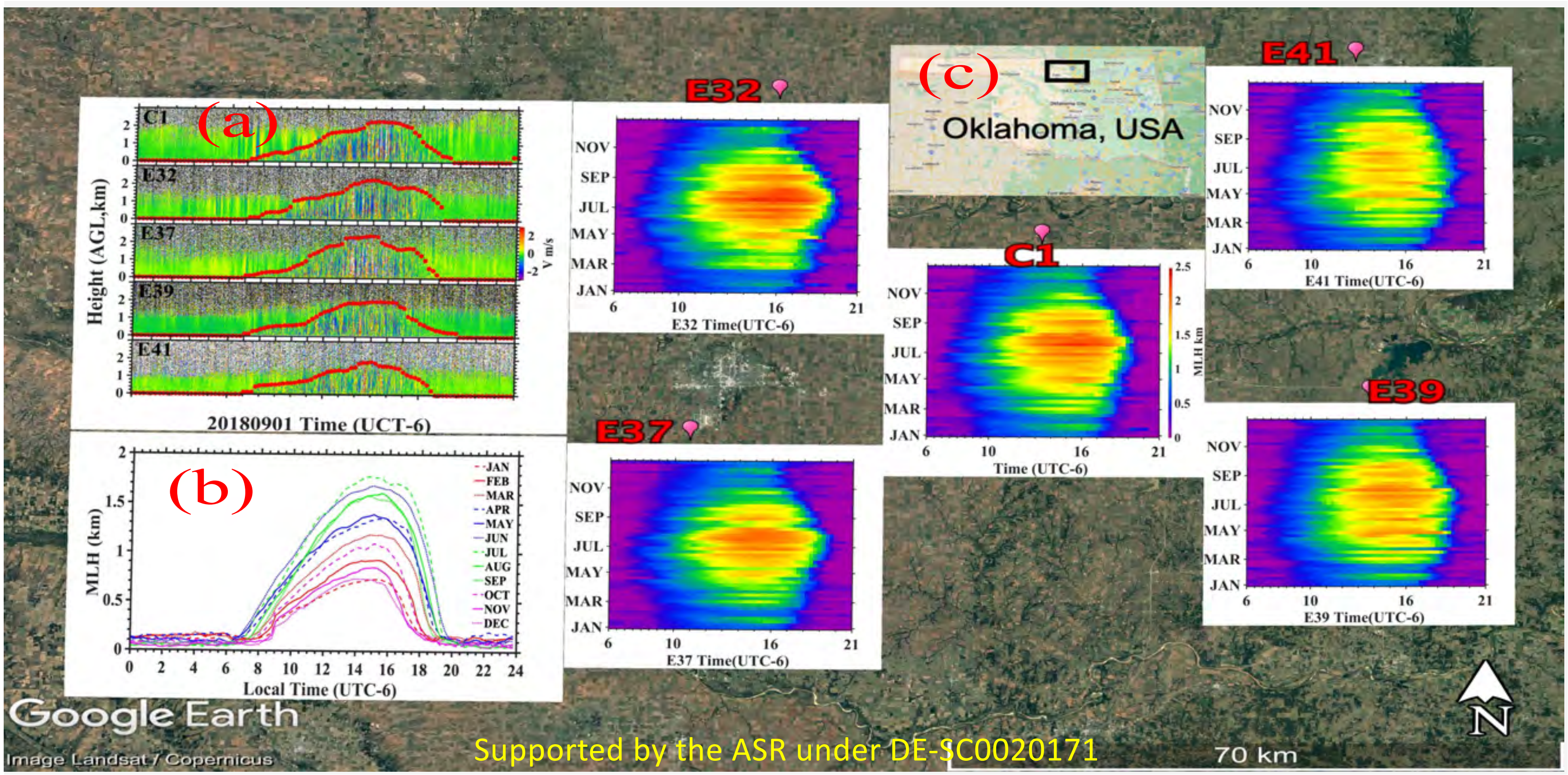

MLH Spatial Variations

- Differences in MLHs over the five sites could be over 50 % of the mean.
- Summer season and afternoon have larger intra-site variations.
- Relative difference are during the starting and decaying periods.
- Large afternoon variations highlight the importance of PBL top entrainment.

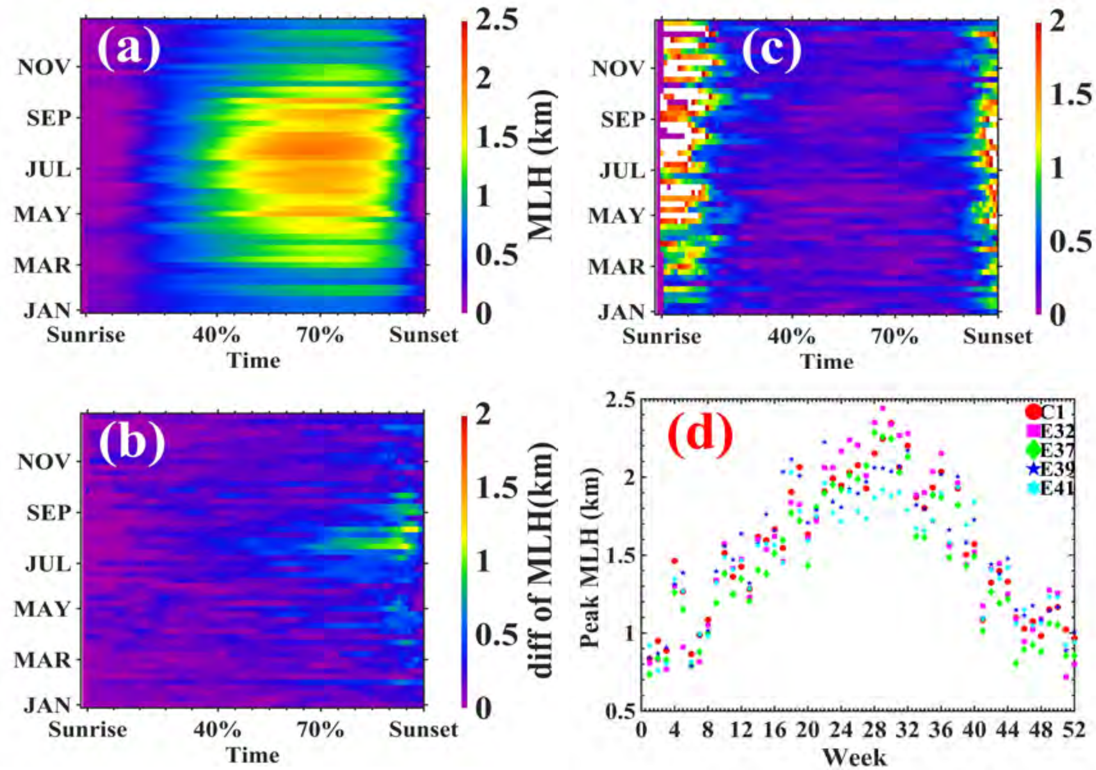

(a) Five-site mean ML height; (b) Maximum difference (highest MLH minus lowest MLH; (c) Difference ratio of ML height ((highest MLH minus lowest MLH)/mean MLH); (d) the peak MLH for every site.

Factors Controlling MLH Developments

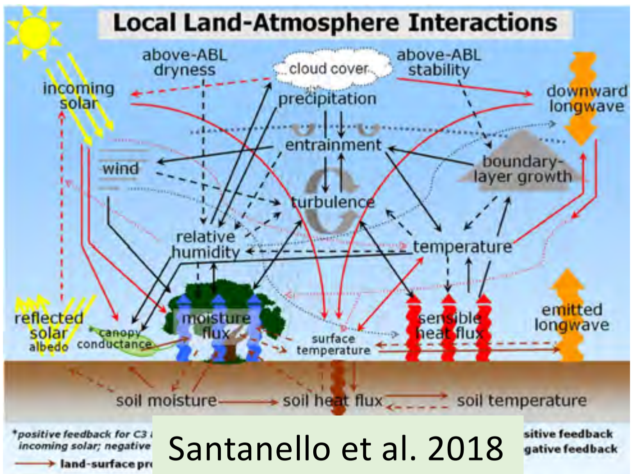

Santanello et al. 2018

- ➢ LTS (low tropospheric stability) dependency indicates that the nocturnal BL has a strong control of convective mixing layer development.
- ➢ Under the same LTS, MLH dependencies on energy supply vary among four sites.

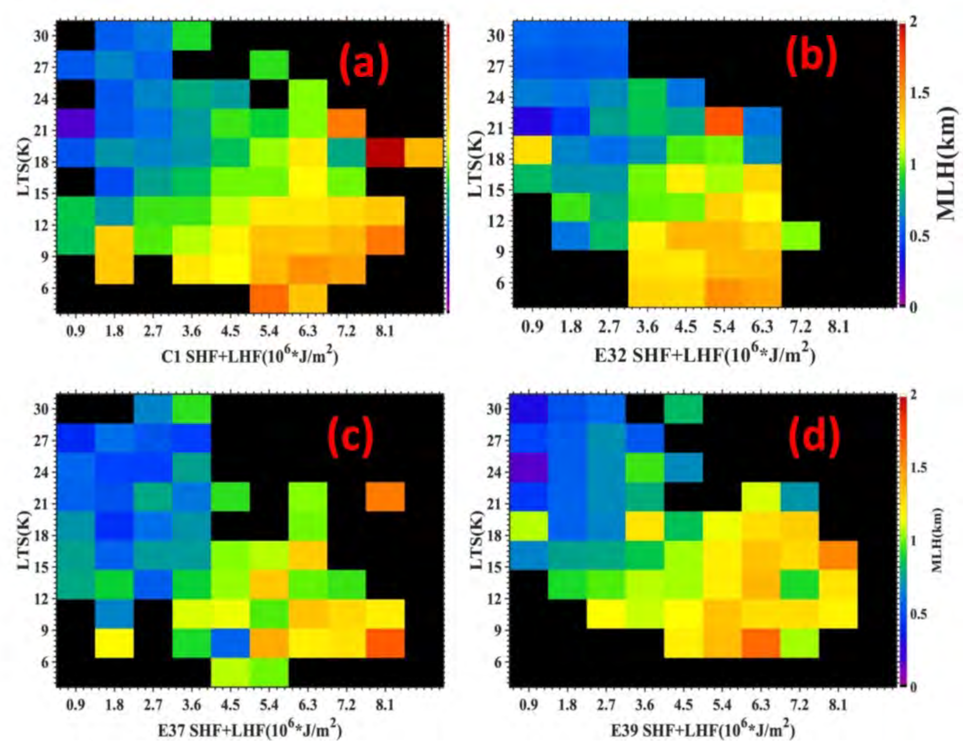

MLH at 11:30 am as a function of LTS and Integrated Energy Supplies

NWP-Based Large-Scale Forcing Impacts on Real-Case LES
Statistical Analysis of LASSO LES

Hyeyum (Hailey) Shin[1], Lulin Xue[1], Zhien Wang[2], Weiwei Li[1], Yufei Chu[2], and William I. Gustafson Jr.[3] ([1]NCAR, [2]CU-Boulder, [3]PNNL)

- **Backgrounds**
  - **Uncertainty in NWP-based large-scale forcing (LSF) is carried over to fine-scale simulations** (e.g., Gustafson et al. 2020)
  - **Large-scale environmental conditions control PBL and convective clouds developments** (e.g., Donner & Phillips 2003; Zhang & Klein 2010, 2013)
- **Objectives**
  1) **Identify key meteorological parameters that lead to the most/least skillful prediction** of the continental shallow cumulus (ShCu) convection over the Southern Great Plains
  2) **Compare performance of different LASSO LSF sources** in prediction of the key parameters
- **DOE LASSO DATA** Gustafson et al. (2020)
  - **100-m LES** driven by NWP-based LSF
  - **82 ShCu cases** in 2016-2019 warm seasons observed over the SGP
  - **8 LSF sources** (including no LSF) for each case
- **Analysis**
  - Bulk PBL and cloud parameters
  - Large-scale environmental conditions

  1) Group by prediction skills
  2) Group by LSF sources

1) Cloud Prediction Skills

- **28% of low skill simulations produce deep convection**; only 3% of high skill simulations predict deep convection.
- **Differences are noticeable only when Deep Cu is simulated**.

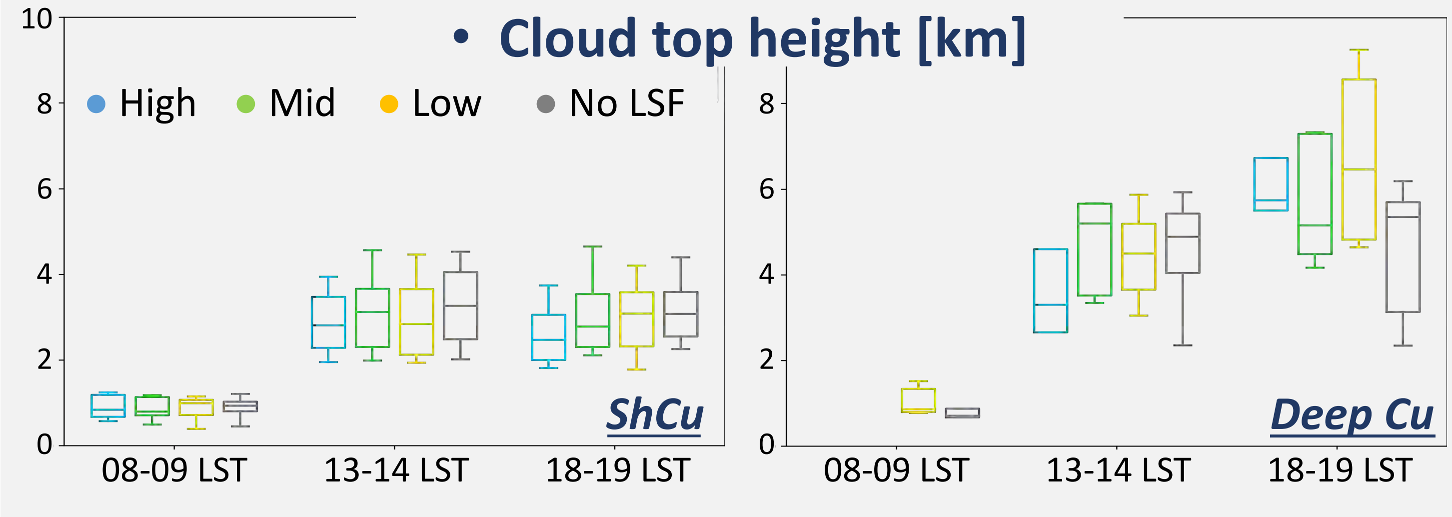

2) Large-Scale Forcing Sources

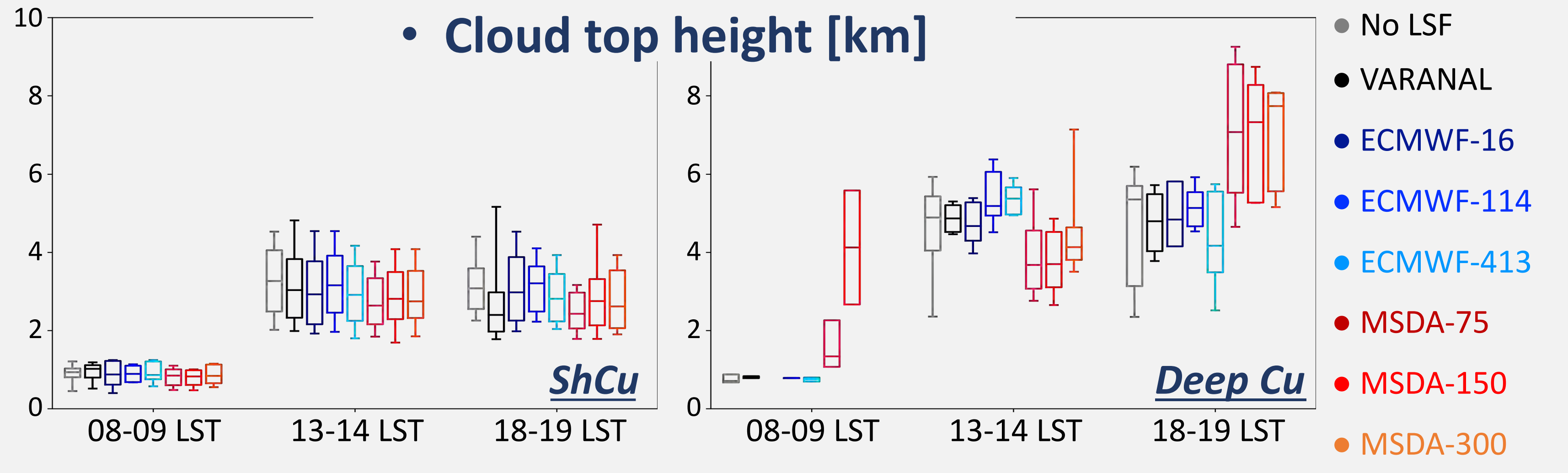

- **Humidity in the lower free troposphere [%]**

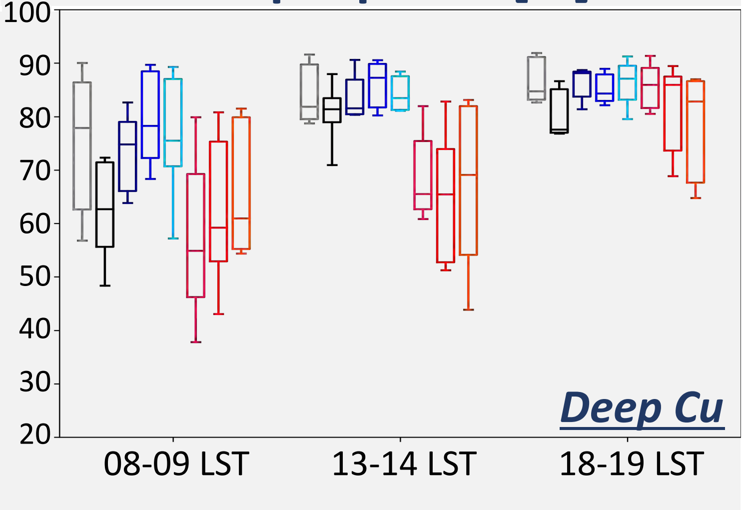

- Differences in simulated deep convection is related to early morning inversion and RH in the lower free troposphere after early morning.

Quantifying the contributions from the surface, advection, and entrainment on the evening transition at SGP

Siwei He (siwei.he@noaa.gov), David D. Turner, Joseph B. Olson, Stanley G. Benjamin, Tatiana G. Smirnova, and Tilden Meyers

NOAA Global System Laboratory
CIRES, University of Colorado Boulder

October 27, 2022

Afternoon to evening transition

- ABL is directly influenced by land surface
- SBL → CBL → SBL → CBL …
- Afternoon to evening transition is the short period before sunset.

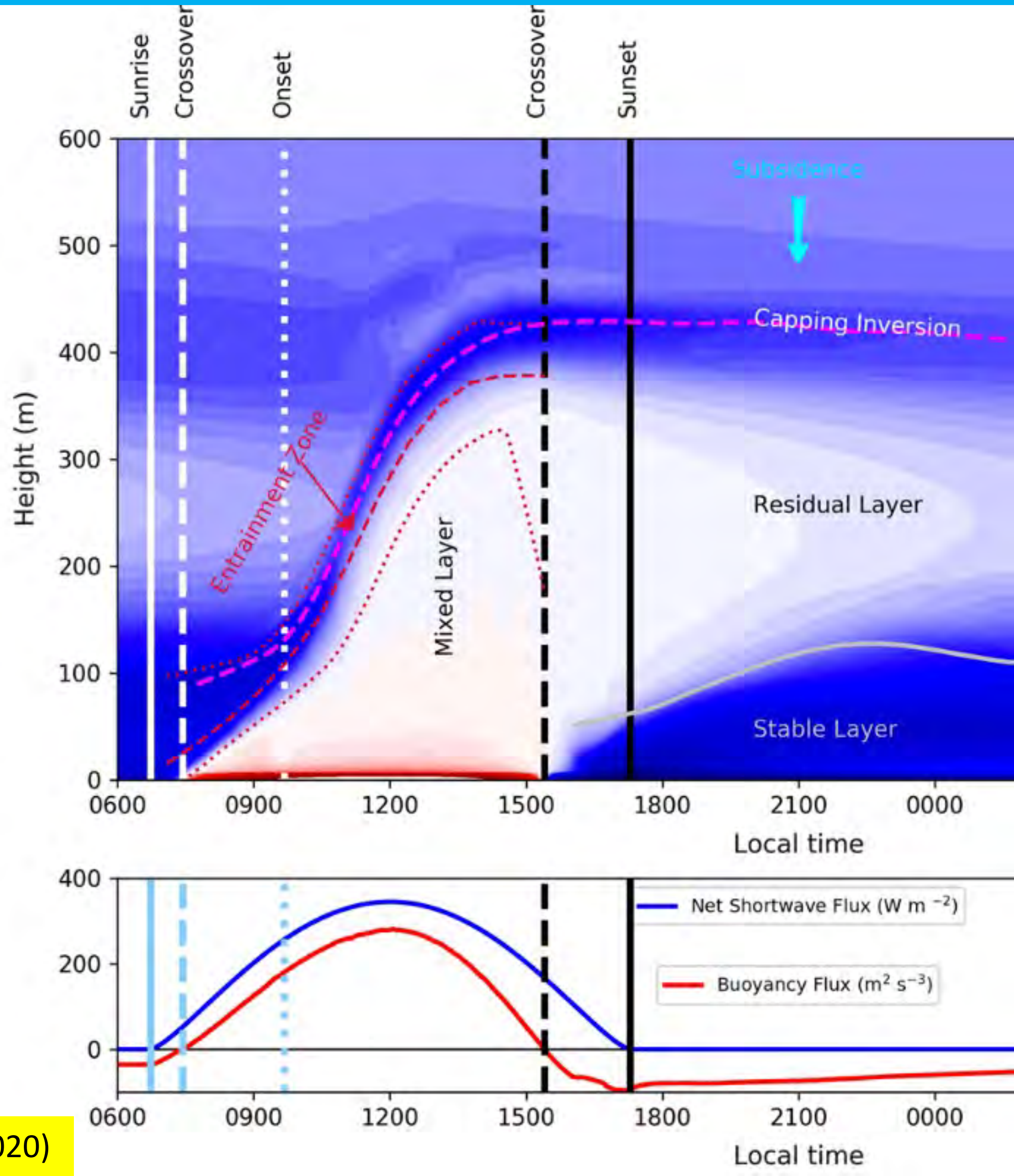

From Angevine et al. (2020)

Afternoon to evening transition

- ABL is directly influenced by land surface
- SBL → CBL → SBL → CBL …
- Afternoon to evening transition is the short period before sunset.
- Previous studies found that:
  - Water vapor increase
  - Temperature drop
  - Wind speed decay

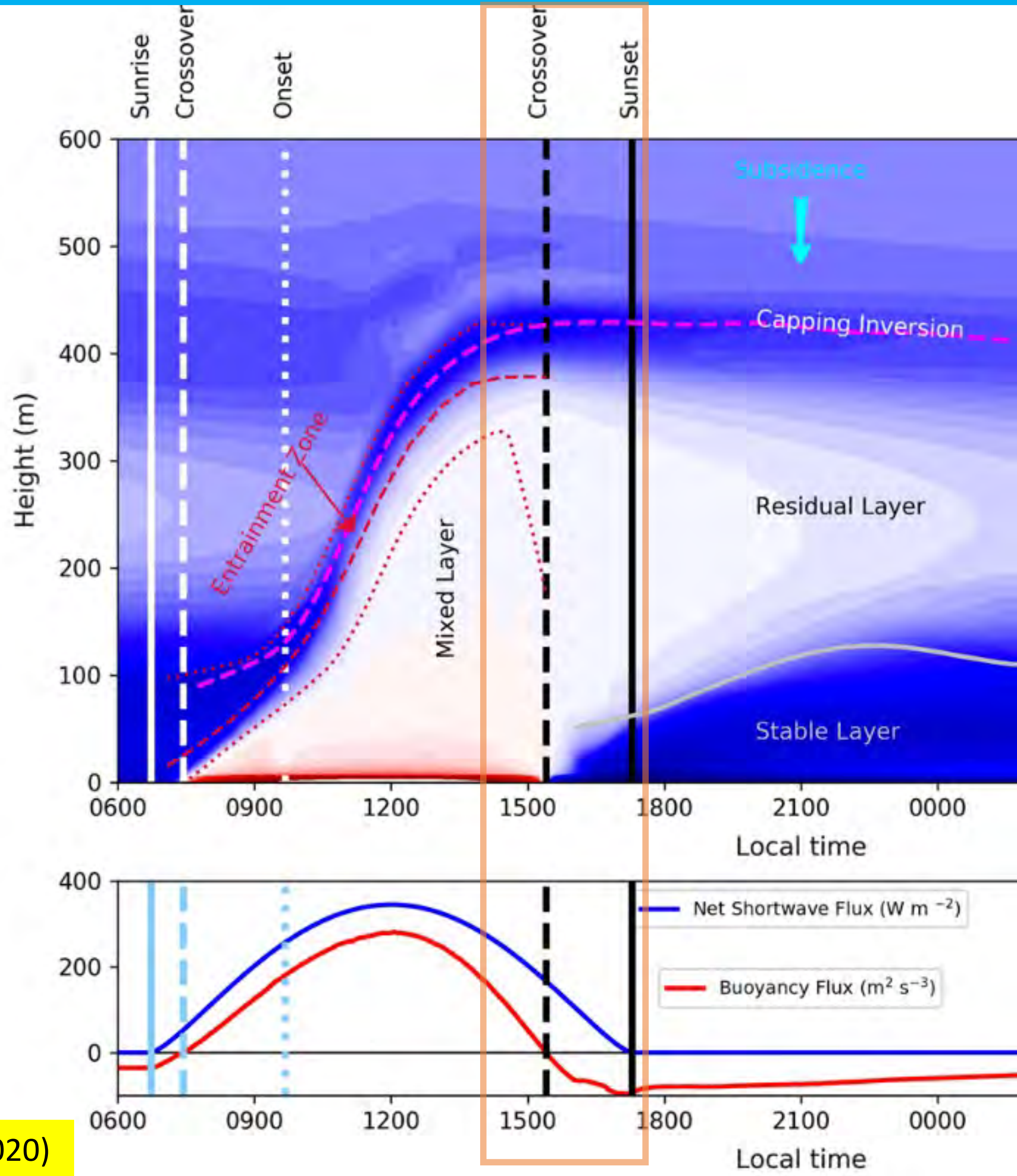

From Angevine et al. (2020)

Afternoon to evening transition

- 2-m mixing ratio diurnal variations over different months and sites, 3-years in-situ observations

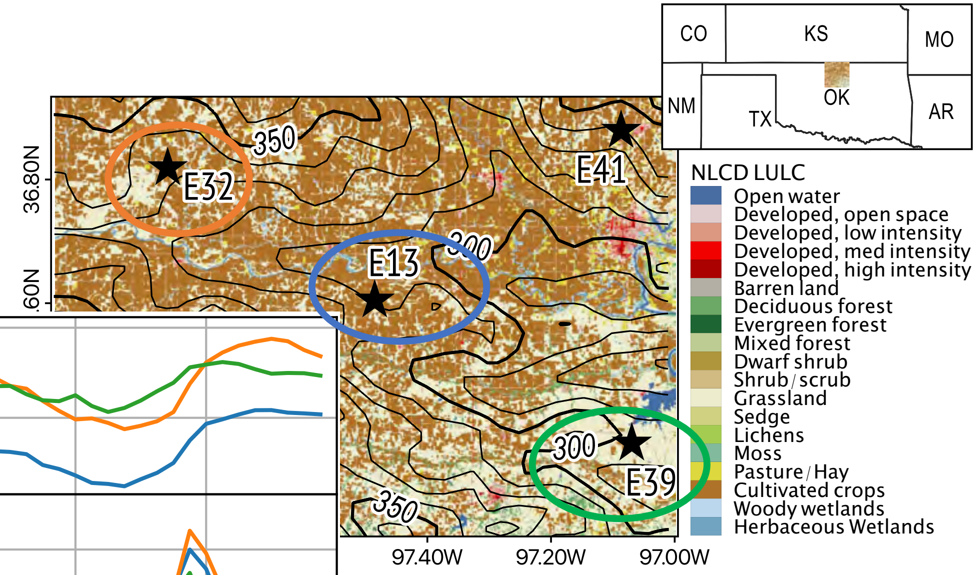

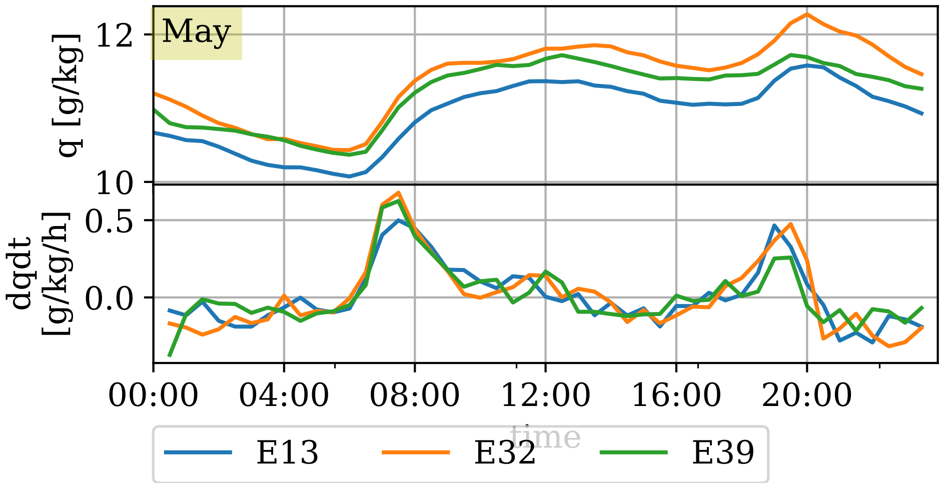

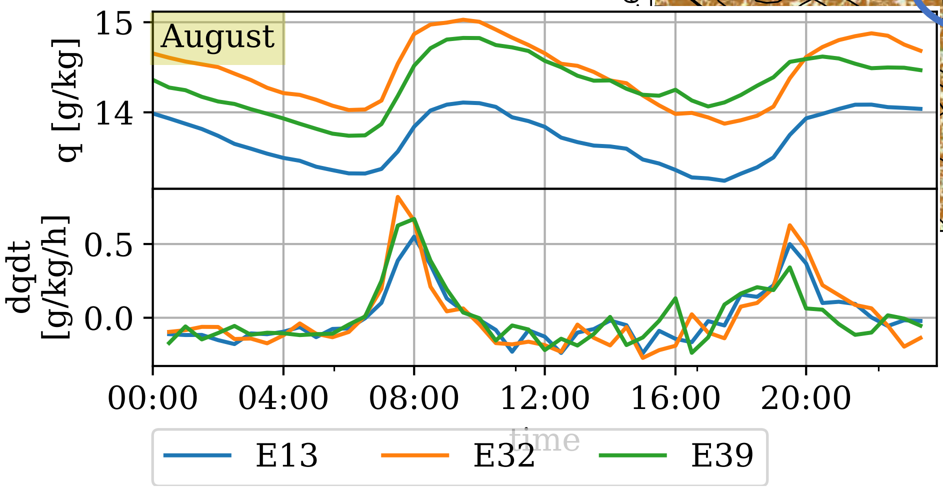

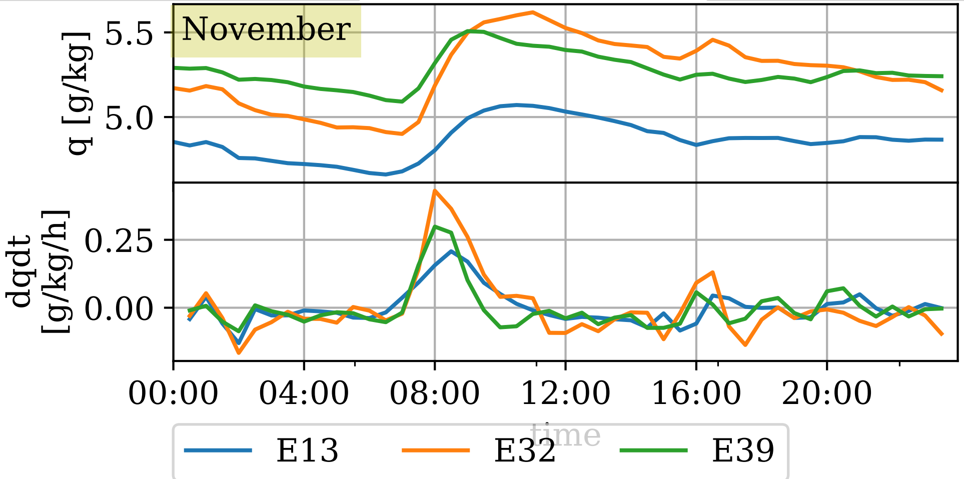

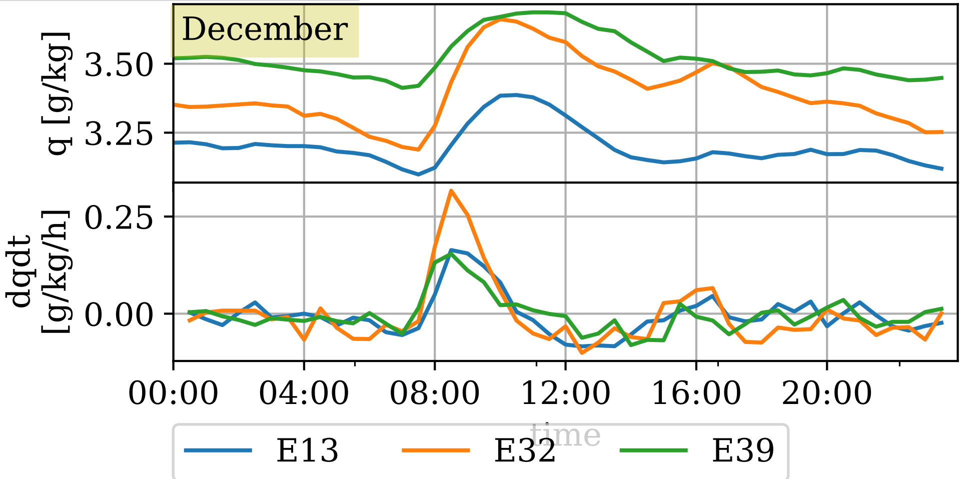

Afternoon to evening transition

- The moisture increase is due to evapotranspiration from the surface.
- The moisture increase is due to water vapor advection.
- The moisture is transported from higher in the CBL towards the surface.

$$\frac{\partial \bar{q}}{\partial t} + \overline{U_j}\frac{\partial \bar{q}}{\partial x_j} = \frac{S_q}{\overline{\rho_{air}}} - \frac{\partial \overline{u_j' q'}}{\partial x_j}$$

Unified Forecast System (UFS) Single Column Model

- The UFS (https://ufscommunity.org/) is a community-based, coupled, comprehensive Earth modeling system.
- Physics:
  - MYNN-EDMF boundary layer and shallow cloud scheme
  - MYNN surface layer scheme
  - RUC land surface model
- Initial and Forcing:
  - NOAA rapid refresh (RAP) analysis data
- Vertical layer = 128
- Time step = 150 seconds
- Several clear-sky days were selected

Results

Observations | Simulations

May 13, 2019

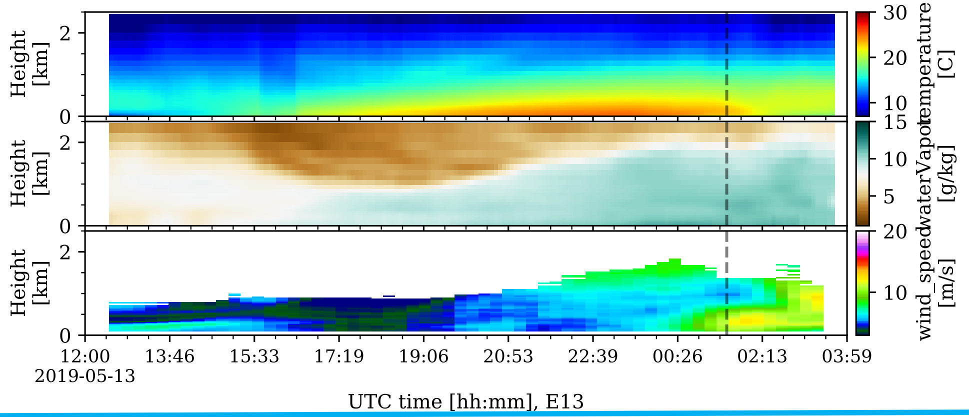

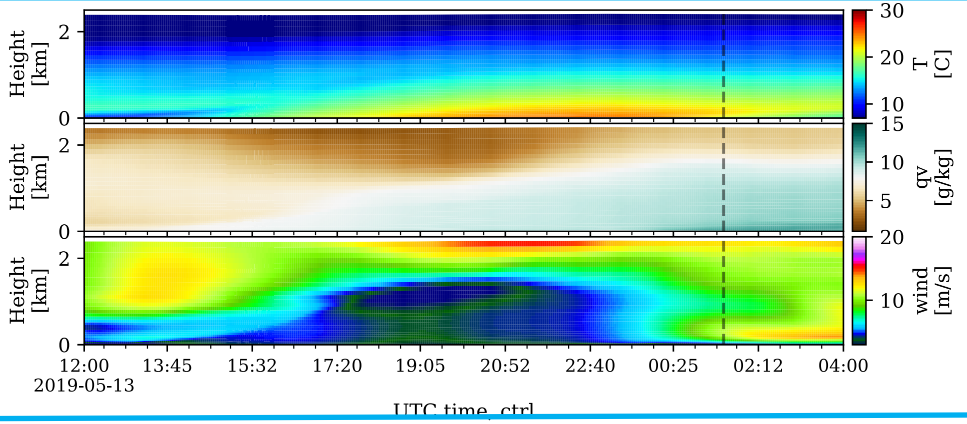

May 15, 2019

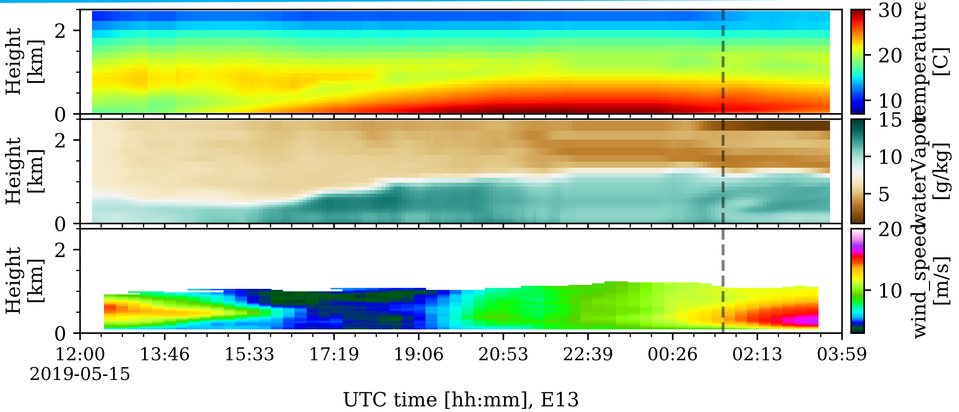

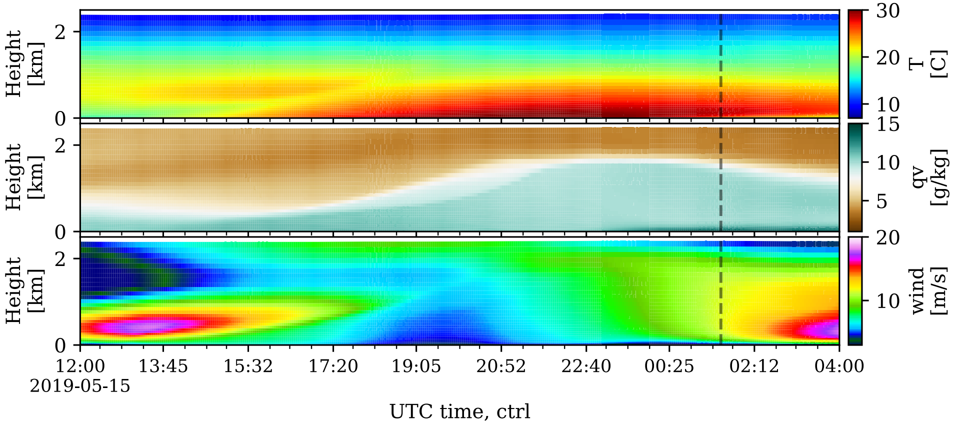

May 16, 2019

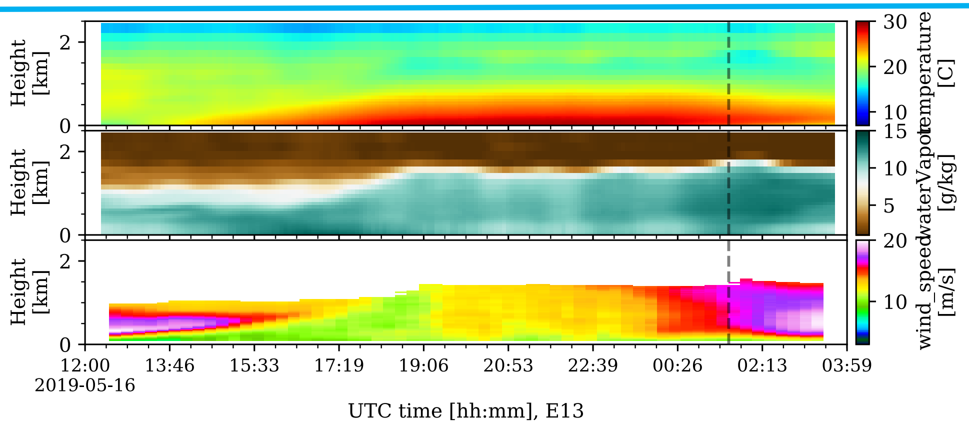

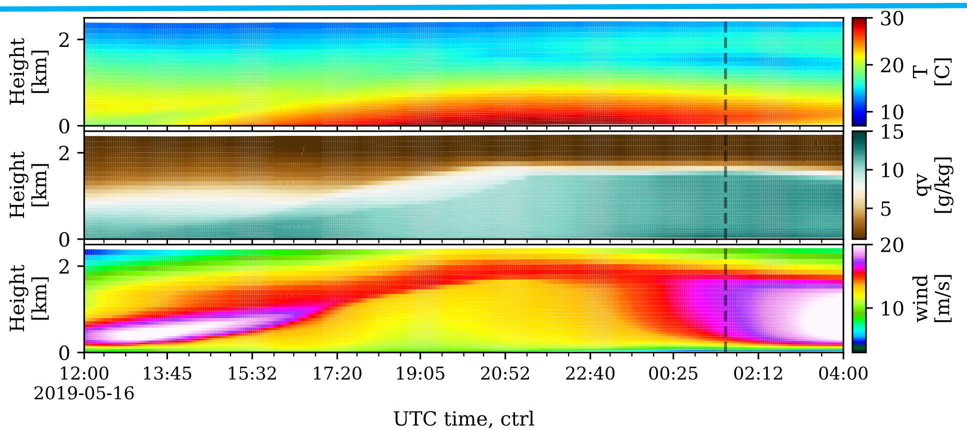

Results

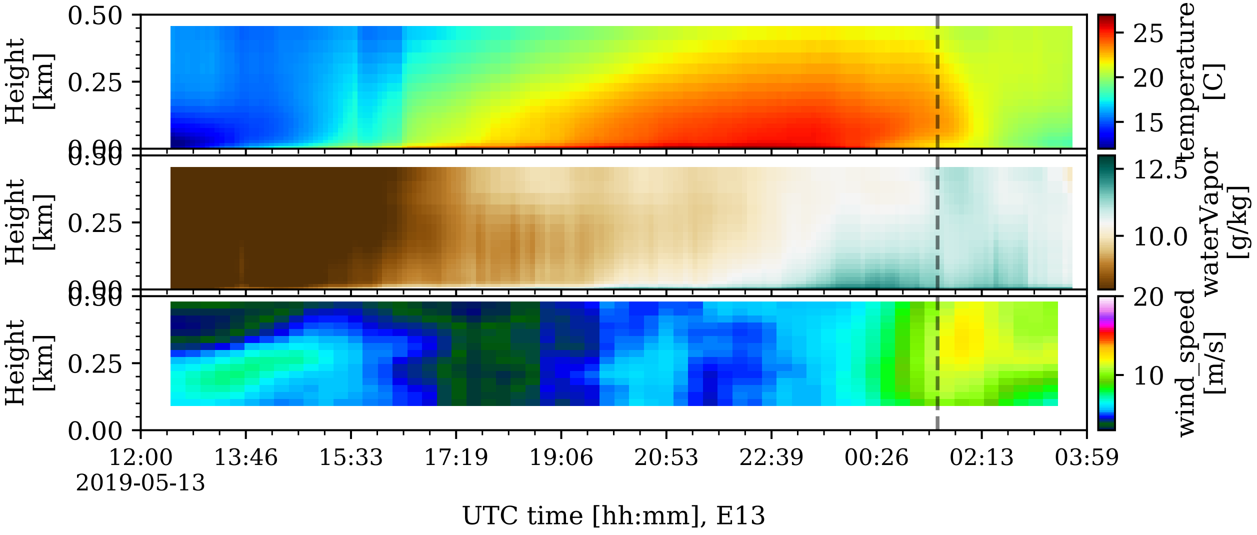

Observations, May 13, 2019

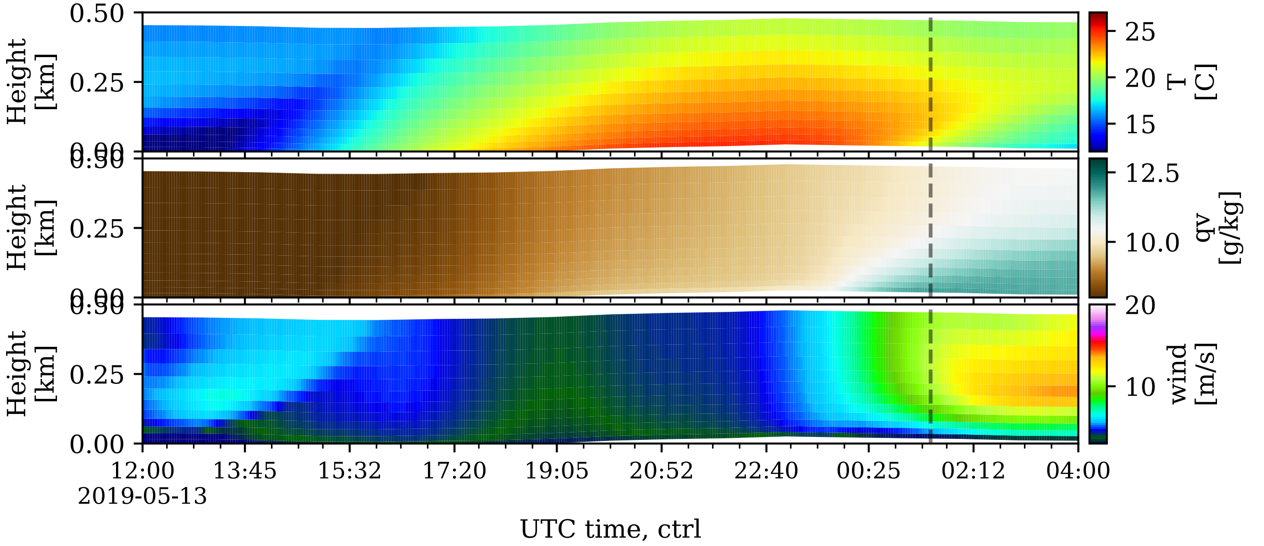

Simulations, May 13, 2019

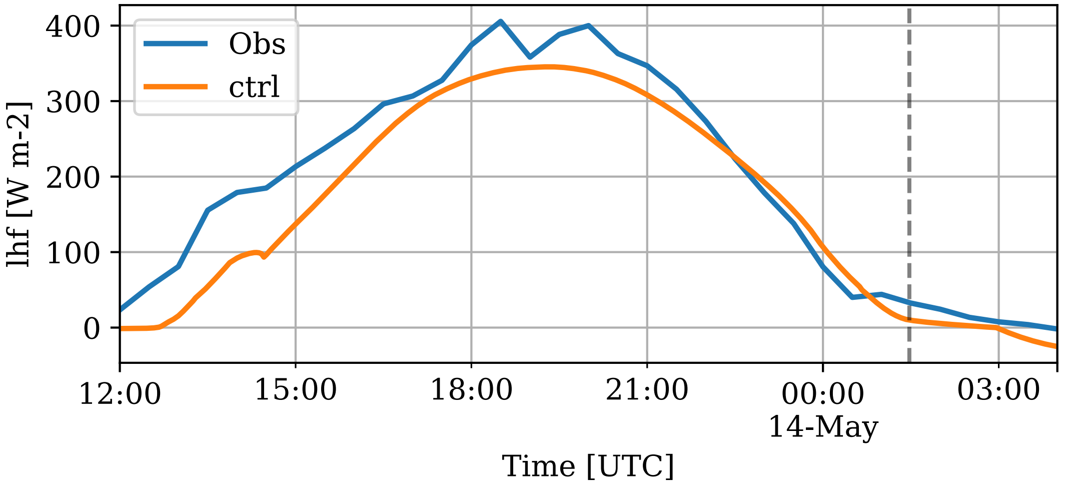

Latent heat flux, May 13, 2019

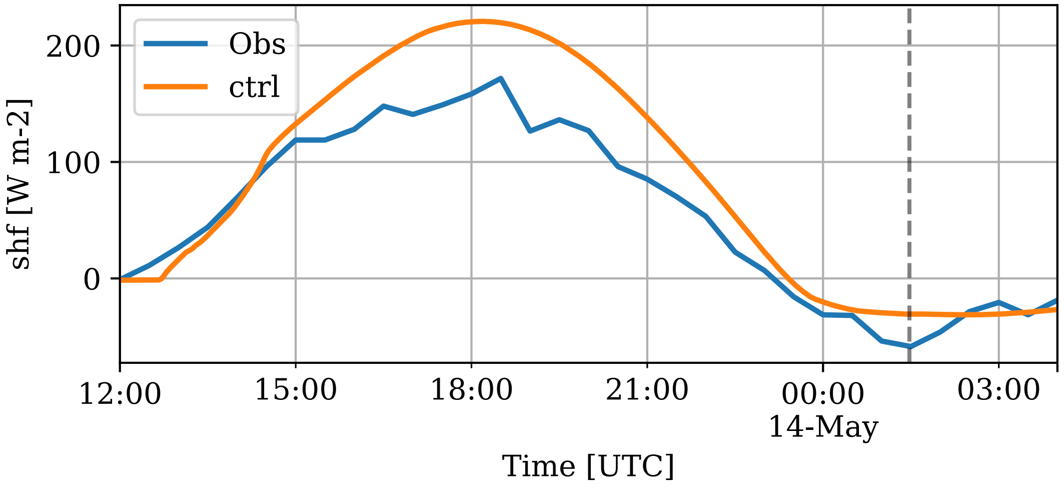

Sensible heat flux, May 13, 2019

Results

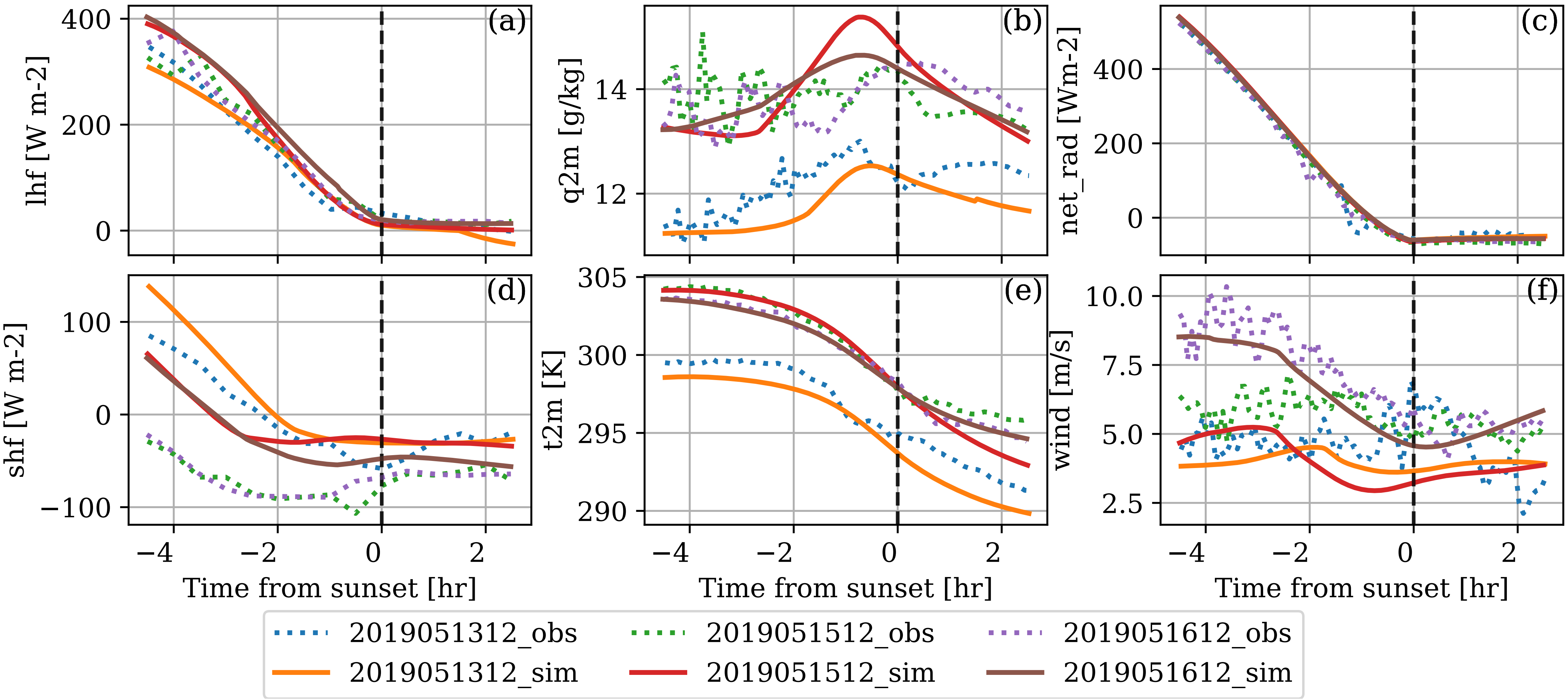

Near-surface variables from the three cases in May, 2019

Results

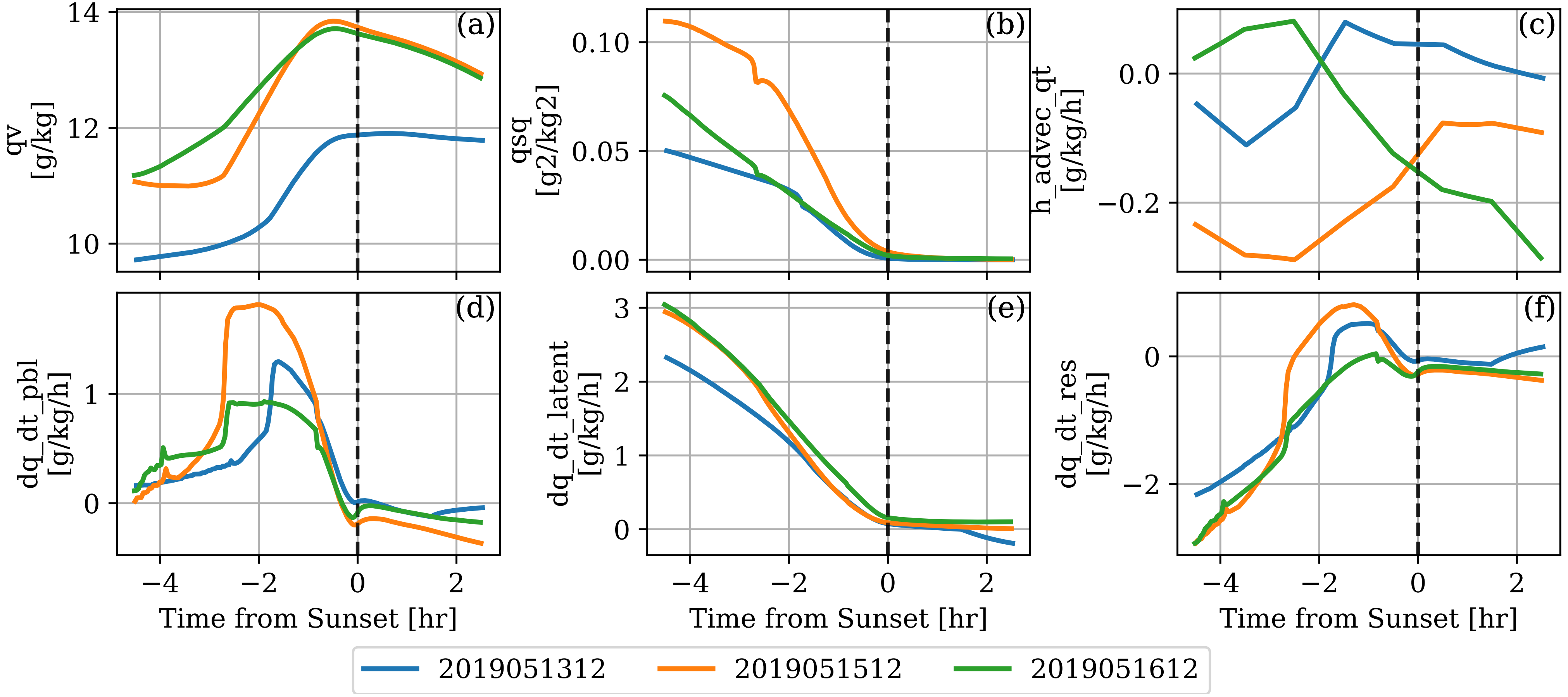

Simulated water vapor related variables of the first bottom layer

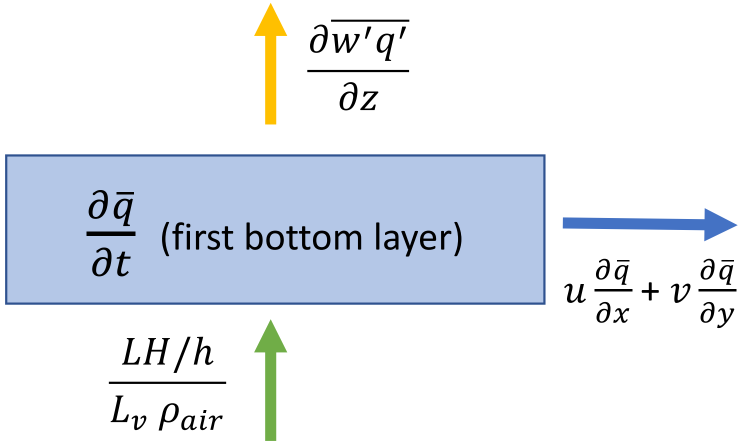

Results

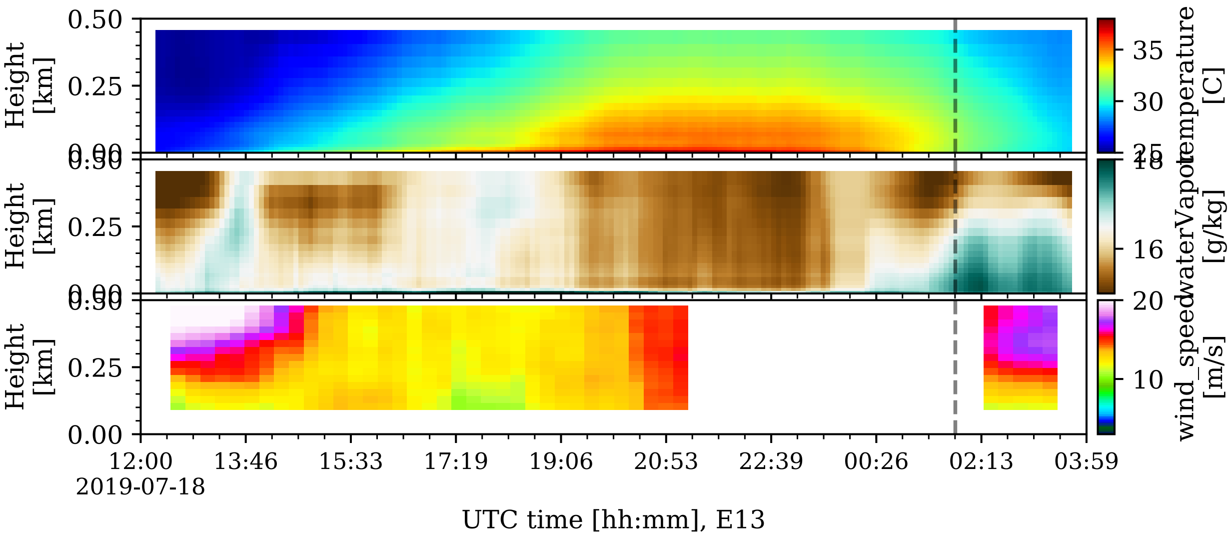

Observations, July 18, 2019

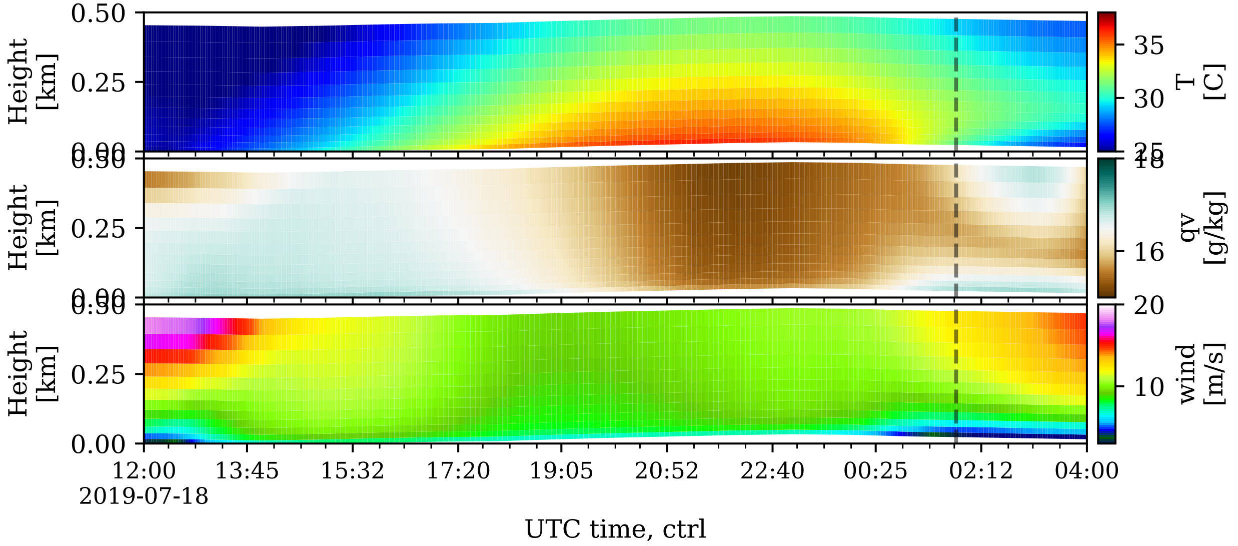

Simulations, July 18, 2019

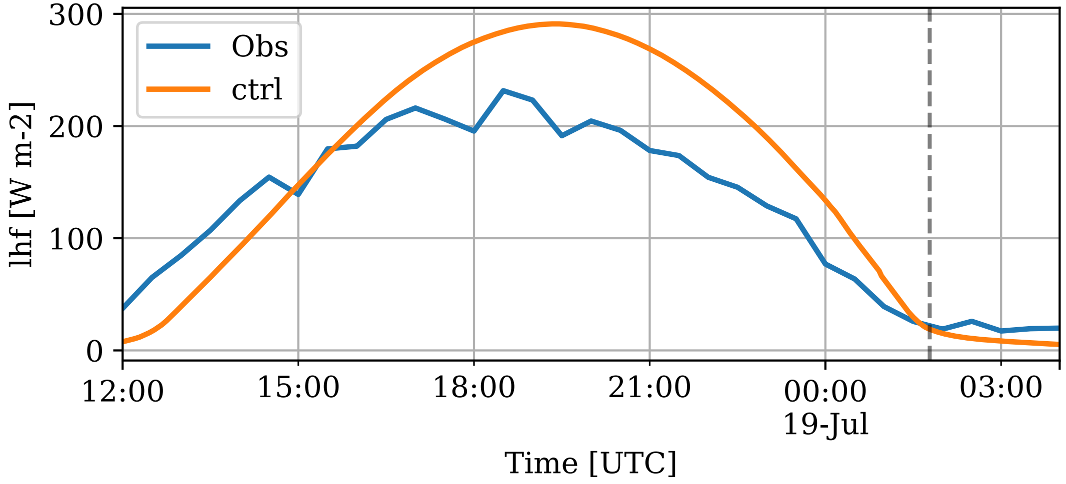

Latent heat flux, July 18, 2019

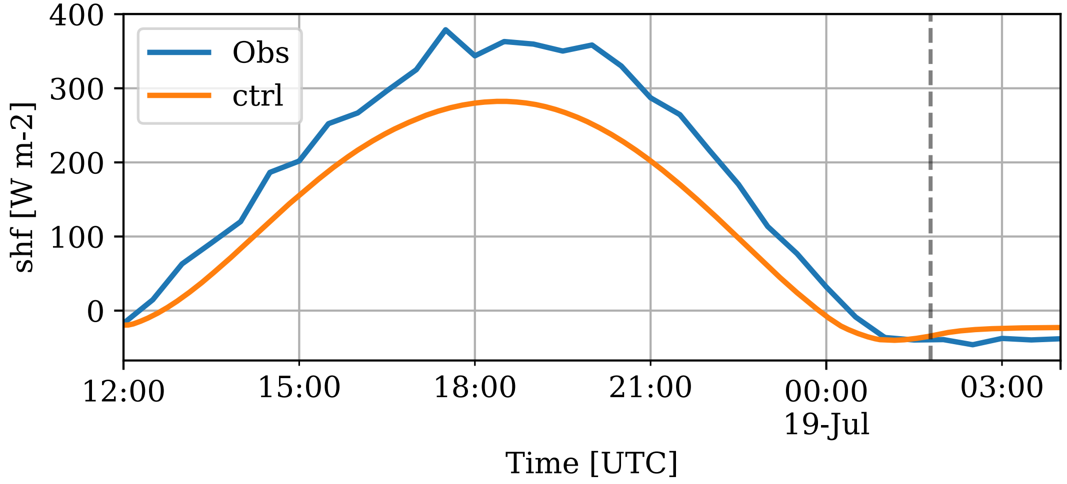

Sensible heat flux, July 18, 2019

Results

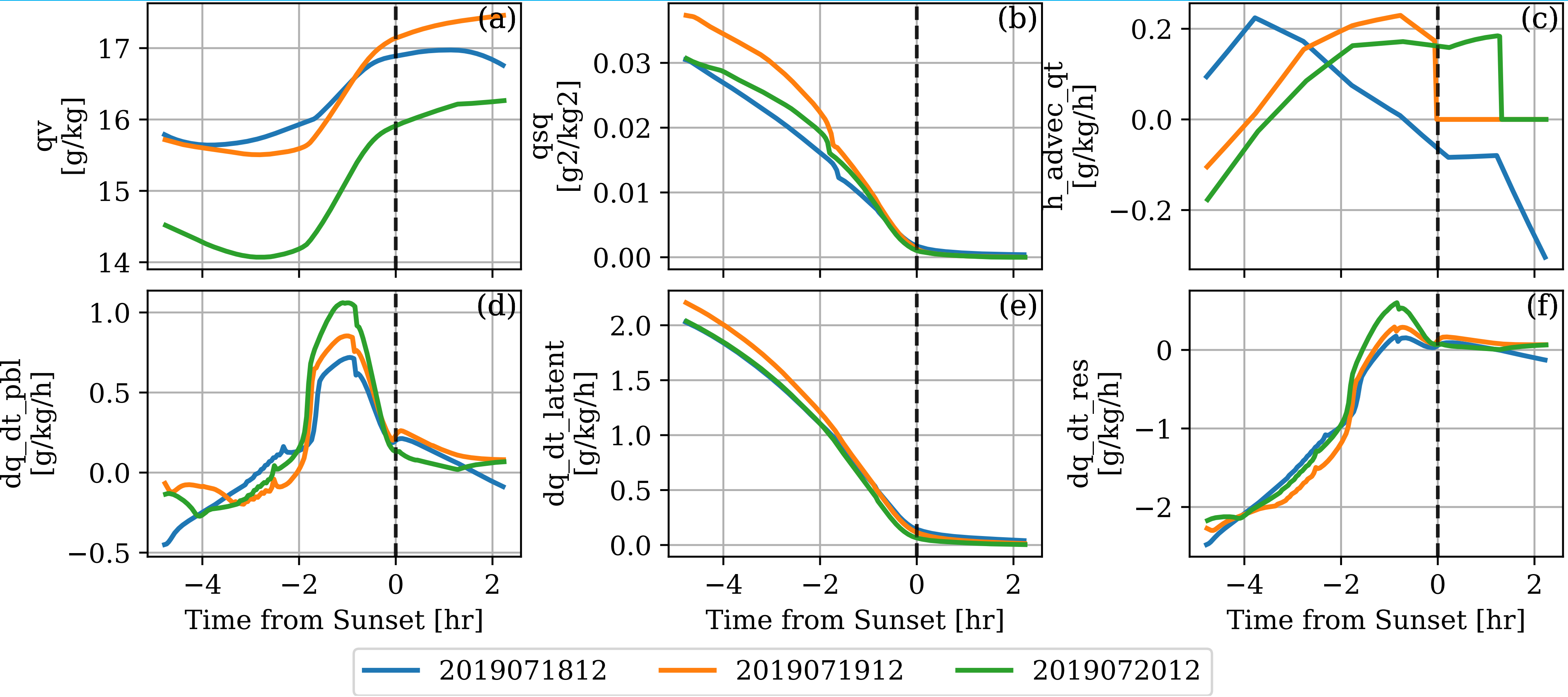

Simulated water vapor related variables of the first bottom layer

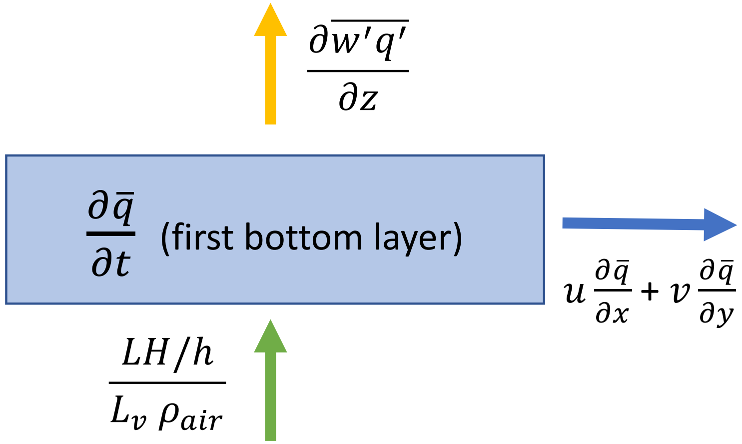

Thank you!